

DF Louvain: Fast Incrementally Expanding Approach for Community Detection on Dynamic Graphs

Subhajit Sahu

subhajit.sahu@research.iiit.ac.in

IIIT Hyderabad

Hyderabad, Telangana, India

ABSTRACT

Community detection is the problem of recognizing natural divisions in networks. A relevant challenge in this problem is to find communities on rapidly evolving graphs. In this report we present our Parallel Dynamic Frontier (DF) Louvain algorithm, which given a batch update of edge deletions and insertions, incrementally identifies and processes an approximate set of affected vertices in the graph with minimal overhead, while using a novel approach of incrementally updating weighted-degrees of vertices and total edge weights of communities. We also present our parallel implementations of Naive-dynamic (ND) and Delta-screening (DS) Louvain. On a server with a 64-core AMD EPYC-7742 processor, our experiments show that DF Louvain obtains speedups of 179 \times , 7.2 \times , and 5.3 \times on real-world dynamic graphs, compared to Static, ND, and DS Louvain, respectively, and is 183 \times , 13.8 \times , and 8.7 \times faster, respectively, on large graphs with random batch updates. Moreover, DF Louvain improves its performance by 1.6 \times for every doubling of threads.

KEYWORDS

Community detection, Parallel Dynamic Louvain algorithm

1 INTRODUCTION

Identifying hidden communities within networks is a crucial graph analytics problem that arises in various domains such as drug discovery, disease prediction, protein annotation, topic discovery, inferring land use, and criminal identification. Here, we want to identify groups of vertices that exhibit dense internal connections but sparse connections with the rest of the graph. These communities are intrinsic when identified based on network topology alone, without external attributes, and they are disjoint when each vertex belongs to only one community [23]. However, the problem is NP-hard, and there is a lack of apriori knowledge on the number and size distribution of communities [7]. To solve this issue, researchers have come up with a number of heuristics for finding communities [7, 14, 15, 17, 22–25, 29, 35, 40, 41, 47, 49–52, 54]. To measure the quality of communities identified, fitness metrics such as the modularity score proposed by Newman et al. [40] are used.

The *Louvain method*, proposed by Blondel et al. [7], is one of the most popular community detection algorithms [31]. It is a greedy, modularity-based optimization algorithm, that hierarchically agglomerates vertices in a graph to obtain communities [7]. It has a time complexity of $O(KM)$ (where M represents the number of edges in the graph, K the total number of iterations performed across all passes), and it efficiently identifies communities with resulting high modularity. A number of algorithmic improvements to the Louvain algorithm have been proposed [2, 18, 21,

26, 34, 38, 44, 53, 55, 59, 62, 64, 65, 71, 74]. To parallelize the algorithm on multicore CPUs [16, 26, 45, 60, 61], GPUs [38], CPU-GPU hybrids [6, 37], multi-GPUs [9, 12, 19, 28], and multi-node systems [5, 20, 21, 57], a number of strategies have been attempted [5, 6, 9, 16, 21, 26, 37, 38, 46, 59, 66, 73].

However, many real-world graphs rapidly evolve with time, through the insertion/deletion of edges/vertices. A growing number of research efforts have focused on detecting communities in dynamic networks [1, 3, 11, 13, 27, 36, 58, 70, 72, 75]. A suitable dynamic approach should identify and process only a subset of vertices that are likely to change their community membership. Note that if the subset of the graph identified as *affected* is too small, we may end up with inaccurate communities, and if it is too large, we incur significant computation time. Hence, one should look to identify an approximate affected set of vertices that covers most of the true affected set of vertices as possible. In addition, determining the vertices to be processed should have low overhead [48].

However, a critical examination of the extant literature on dynamic community detection algorithms indicates a few shortcomings. Some of these algorithms [13, 36] do not outperform static algorithms even for modest-sized batch updates. Aynaud et al. [3] and Chong et al. [11] adapt the existing community labels and run an algorithm, such as Louvain, on the entire graph. Often, this is unwarranted since not every vertex would need to change its community on the insertion/deletion of a few edges. Cordeiro et al. [13] do not consider the cascading impact of changes in community labels, where the community label of a vertex changes because of a change in the community label of its neighbor. Zarayeneh et al. [72] identify a subset of vertices whose community labels are likely to change on the insertion/deletion of a few edges. However, as this set of vertices identified is large, the algorithm of Zaranayeh et al. incurs a significant computation time. Moreover, most of the reported algorithms [3, 11, 13, 36, 72, 75] are sequential. There is thus a pressing need for efficient parallel algorithms for community detection on large dynamic graphs. Further, none of the works recommend reusing the previous *total edge weight* of each vertex/community (required for local-moving phase of Louvain algorithm) as auxiliary information to the dynamic algorithm. Recomputing it from scratch is expensive and becomes a bottleneck for dynamic Louvain algorithm. Table 1 summarizes the above discussion.

This technical report introduces our Parallel Dynamic Frontier (DF) Louvain,¹ which given a batch update, efficiently identifies and processes affected vertices with minimal overhead, while incrementally updating weighted-degrees of vertices and total edge weights of communities, which significantly improves its performance.

¹<https://github.com/puzzlef/louvain-communities-openmp-dynamic>

Table 1: A comparison of the properties of dynamic community detection approaches.

Approach	Published	Fully dynamic	Batch update	Process subset	Use auxiliary info.	Parallel algorithm
Aynaud et al. [3]	2010	✓	✓	×	×	×
Chong et al. [11]	2013	✓	✓	×	×	×
Meng et al. [36]	2016	✓	✓	×	×	×
Cordeiro et al. [13]	2016	✓	✓	×	×	×
Zarayeneh et al. [72]	2021	✓	✓	✓	×	×
Ours	2024	✓	✓	✓	✓	✓

2 RELATED WORK

A core idea for dynamic community detection, among most approaches, is to use the community membership of each vertex from the previous snapshot of the graph, instead of initializing each vertex into singleton communities [3, 11, 13, 72]. Aynaud et al. [3] simply run the Louvain algorithm after assigning the community membership of each vertex as its previous community membership. Chong et al. [11] reset the community membership of vertices linked to an updated edge, in addition to the steps performed by Aynaud et al., and process all vertices with the Louvain algorithm.

Meng et al. [36] present a dynamic Louvain algorithm with an objective of obtaining temporally smoothed community structures as the graphs evolve over time. To avoid dramatic changes in community structure, they use an approximate version of delta-modularity optimization. This approximate formulation relies on both graphs in the previous and the current snapshot with a user-defined ratio. Their algorithm demonstrates improvement over Dynamic Spectral Clustering (DSC) [10] and Multi-Step Community Detection (MSCD) [4] in terms of runtime. In terms of quality of communities obtained (using modularity score), their algorithm outperforms DSC, and is on par with MSCD.

Cordeiro et al. [13] propose a dynamic algorithm with a similar objective, i.e., tracking communities over time. Their algorithm performs a local modularity optimization that maximizes the modularity gain function only for those communities where the editing of nodes and edges was performed by disbanding such communities to a lower-level network, keeping the rest of the network unchanged. They confirm supremacy of their algorithm over LabelRank [69], LabelRankT [67], Speaker-Listener Label Propagation (SLPA) [68], and Adaptive Finding Overlapping Community Structure (AFOCS) [42] in terms of runtime – and over LabelRank, LabelRankT and AFOCS in terms of modularity score.

Zarayeneh et al. [72] propose the Delta screening approach for updating communities in a dynamic graph. This technique examines edge deletions and insertions to the original graph, and identifies a subset of vertices that are likely to be impacted by the change using the modularity objective. Subsequently, only the identified subsets are processed for community state updates – using two modularity optimization based community detection algorithms, Louvain and Smart Local-Moving (SLM). Their results demonstrate performance improvement over the Static Louvain algorithm, and a dynamic baseline version of Louvain algorithm [3]. They also compare the performance of their algorithm against two other state-of-the-art methods DynaMo [75] and Batch [11], and observe improvement over the methods both in terms of runtime and modularity.

3 PRELIMINARIES

Let $G(V, E, w)$ be an undirected graph, with V as the set of vertices, E as the set of edges, and $w_{ij} = w_{ji}$ a positive weight associated with each edge in the graph. If the graph is unweighted, we assume each edge to be associated with unit weight ($w_{ij} = 1$). Further, we denote the neighbors of each vertex i as $J_i = \{j \mid (i, j) \in E\}$, the weighted degree of each vertex i as $K_i = \sum_{j \in J_i} w_{ij}$, the total number of vertices in the graph as $N = |V|$, the total number of edges in the graph as $M = |E|$, and the sum of edge weights in the undirected graph as $m = \sum_{i, j \in V} w_{ij}/2$.

3.1 Community detection

Disjoint community detection is the process of arriving at a community membership mapping, $C : V \rightarrow \Gamma$, which maps each vertex $i \in V$ to a community-id $c \in \Gamma$, where Γ is the set of community-ids. We denote the vertices of a community $c \in \Gamma$ as V_c . We denote the community that a vertex i belongs to as C_i . Further, we denote the neighbors of vertex i belonging to a community c as $J_{i \rightarrow c} = \{j \mid j \in J_i \text{ and } C_j = c\}$, the sum of those edge weights as $K_{i \rightarrow c} = \{w_{ij} \mid j \in J_{i \rightarrow c}\}$, the sum of weights of edges within a community c as $\sigma_c = \sum_{(i, j) \in E \text{ and } C_i=C_j=c} w_{ij}$, and the total edge weight of a community c as $\Sigma_c = \sum_{(i, j) \in E \text{ and } C_i=c} w_{ij}$ [32, 72].

3.2 Modularity

Modularity is a fitness metric that is used to evaluate the quality of communities obtained by community detection algorithms (as they are heuristic based). It is calculated as the difference between the fraction of edges within communities and the expected fraction of edges if the edges were distributed randomly. It lies in the range $[-0.5, 1]$ (higher is better) [8]. Optimizing this function theoretically leads to the best possible grouping [39, 63].

We can calculate the modularity Q of obtained communities using Equation 1, where δ is the Kronecker delta function ($\delta(x, y) = 1$ if $x = y$, 0 otherwise). The *delta modularity* of moving a vertex i from community d to community c , denoted as $\Delta Q_{i:d \rightarrow c}$, can be calculated using Equation 2.

$$Q = \frac{1}{2m} \sum_{(i, j) \in E} \left[w_{ij} - \frac{K_i K_j}{2m} \right] \delta(C_i, C_j) = \sum_{c \in \Gamma} \left[\frac{\sigma_c}{2m} - \left(\frac{\Sigma_c}{2m} \right)^2 \right] \quad (1)$$

$$\Delta Q_{i:d \rightarrow c} = \frac{1}{m} (K_{i \rightarrow c} - K_{i \rightarrow d}) - \frac{K_i}{2m^2} (K_i + \Sigma_c - \Sigma_d) \quad (2)$$

3.3 Louvain algorithm

The Louvain method is a greedy, modularity optimization based agglomerative algorithm that finds high quality communities within a graph, with a time complexity of $O(KM)$ (where K is the number of iterations performed across all passes), and a space complexity of $O(N + M)$ [31]. It consists of two phases: the *local-moving phase*, where each vertex i greedily decides to move to the community of one of its neighbors $j \in J_i$ that gives the greatest increase in modularity $\Delta Q_{i:C_i \rightarrow C_j}$ (using Equation 2), and the *aggregation phase*, where all the vertices in a community are collapsed into a single super-vertex. The two phases make up one pass, which repeats until there is no further increase in modularity. As a result, we have a hierarchy of community memberships for each vertex as a dendrogram. The top-level hierarchy is the final result [32].

3.4 Dynamic approaches

A dynamic graph can be denoted as a sequence of graphs, where $G^t(V^t, E^t, w^t)$ denotes the graph at time step t . The changes between graphs $G^{t-1}(V^{t-1}, E^{t-1}, w^{t-1})$ and $G^t(V^t, E^t, w^t)$ at consecutive time steps $t - 1$ and t can be denoted as a batch update Δ^t at time step t which consists of a set of edge deletions $\Delta^{t-} = \{(i, j) \mid i, j \in V\} = E^{t-1} \setminus E^t$ and a set of edge insertions $\Delta^{t+} = \{(i, j, w_{ij}) \mid i, j \in V; w_{ij} > 0\} = E^t \setminus E^{t-1}$ [72]. We refer to the setting where Δ^t consists of multiple edges being deleted and inserted as a *batch update*.

3.4.1 Naive-dynamic (ND) approach. The *Naive-dynamic* approach, originally presented by Aynaud et al. [3], is a simple approach for identifying communities in dynamic networks. Here, one assigns vertices to communities from the previous snapshot of the graph and processes all the vertices, regardless of the edge deletions and insertions in the batch update (hence the prefix *naive*). This is demonstrated in Figure 1(a), where all vertices are marked as affected, highlighted in yellow. Since all communities are also marked as affected, they are all shown as hatched. Note that within the figure, edge deletions are shown in the top row (denoted by dotted lines), edge insertions are shown in the middle row (also denoted by dotted lines), and the migration of a vertex during the community detection algorithm is shown in the bottom row. The community membership obtained through this approach is guaranteed to be at least as accurate as the static algorithm. The pseudocode for our parallel version of this approach is given in Algorithm 2, with its explanation given in Section A.1. It uses weighted-degrees of vertices and total edge weights of communities as auxiliary information.

3.4.2 Delta-screening (DS) approach. *Delta-screening*, proposed by Zarayeneh et al. [72], is a dynamic community detection approach that uses modularity-based scoring to determine an approximate region of the graph in which vertices are likely to change their community membership. Figure 1(b) presents a high-level overview of the vertices (and communities), linked to a single source vertex i , that are identified as affected using the DS approach in response to a batch update involving both edge deletions and insertions. In the DS approach, Zarayeneh et al. first separately sort the batch update consisting of edge deletions $(i, j) \in \Delta^{t-}$ and insertions $(i, j, w) \in \Delta^{t+}$ by their source vertex-id. For edge deletions within the same community, they mark i 's neighbors and j 's community as

affected. For edge insertions across communities, they pick the highest modularity changing vertex j^* among all the insertions linked to vertex i and mark i 's neighbors and j^* 's community as affected. Edge deletions between different communities and edge insertions between the same community are unlikely to affect the community membership of either of the vertices or any other vertices and hence ignored. The affected vertices identified by the DS approach apply to the first pass of Louvain, and the community membership of each vertex is initialized at the start of the community detection algorithm to that obtained in the previous snapshot of the graph. We note that the DS approach, is *not* guaranteed to explore all vertices that have the potential to change their membership [72].

The DS approach, proposed by Zarayeneh et al. [72] is not parallel. In this paper, we translate their approach into a parallel algorithm. To this end, we scan sorted edge deletions and insertions in parallel, apply the DS approach, as mentioned above, and mark vertices, neighbors of a vertex, and the community of a vertex using three separate flag vectors. Finally, we use the neighbors and community flag vectors to mark appropriate vertices. We also use per-thread collision-free hash tables. The pseudocode for our parallel version of the DS approach is given in Algorithm 3, with its explanation given in Section A.2. Similar to our parallel implementation of ND Louvain, it utilizes the weighted-degrees of vertices and the total edge weights of communities as auxiliary information.

4 APPROACH

Given a batch update on the original graph, it is likely that only a small subset of vertices in the graph would change their community membership. Selection of the appropriate set of affected vertices to be processed (that are likely to change their community), in addition to the overhead of finding them, plays a significant role in the overall accuracy and efficiency of a dynamic batch parallel algorithm. Too small a subset may result in poor-quality communities, while a too-large subset will increase computation time. However, the Naive-dynamic (ND) approach processes all the vertices, while the Delta-screening (DS) approach generally overestimates the set of affected vertices and has a high overhead. Our proposed Dynamic Frontier (DF) approach addresses these issues.

4.1 Our Dynamic Frontier (DF) approach

We now explain the *Dynamic Frontier* approach. Consider a batch update consisting of edge deletions $(i, j, w) \in \Delta^{t-}$ and insertions $(i, j, w) \in \Delta^{t+}$, both shown with dotted lines, with respect to a single source vertex i , in Figure 1(c). At the start of the community detection algorithm, we initialize the community membership of each vertex to that obtained in the previous snapshot of the graph.

Initial marking of affected vertices upon edge deletion/insertion. For edge deletions between vertices belonging to the same community and edge insertions between vertices belonging to different communities, we mark the source vertex i as affected, as shown with vertices highlighted in yellow, in Figure 1(c). Note that batch updates are undirected, so we effectively mark both the endpoints i and j . Edge deletions between vertices lying across communities and edge insertions for vertices lying within the same community are ignored (for reasons stated before, in Section 3.4.2).

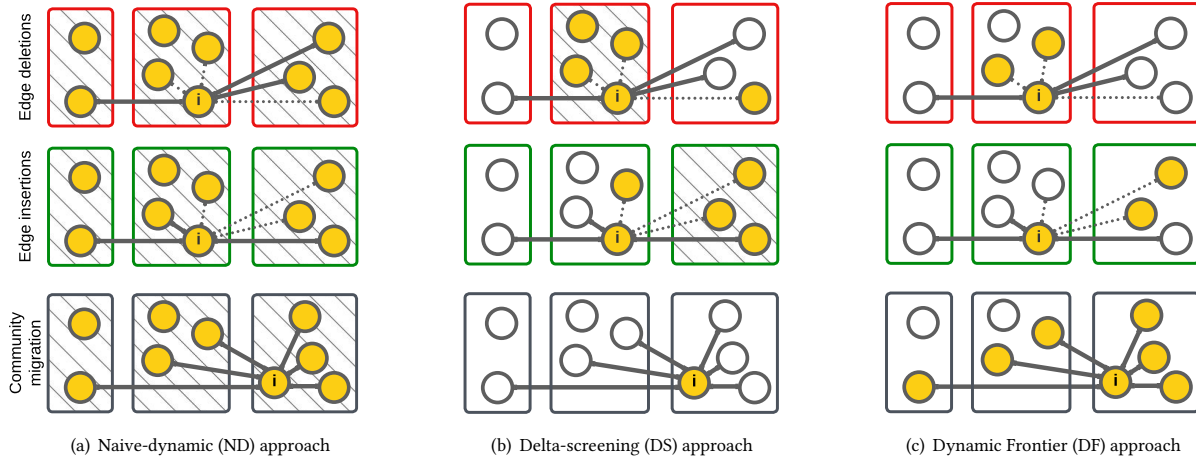


Figure 1: Comparison of dynamic community detection approaches: Naive-dynamic (ND), Delta-screening (DS), and our Dynamic Frontier (DF) approach. Edge deletions/insertions are indicated with dotted lines. Vertices marked as affected (initially) with each approach are highlighted in yellow, and when entire communities are marked as affected, they are hatched.

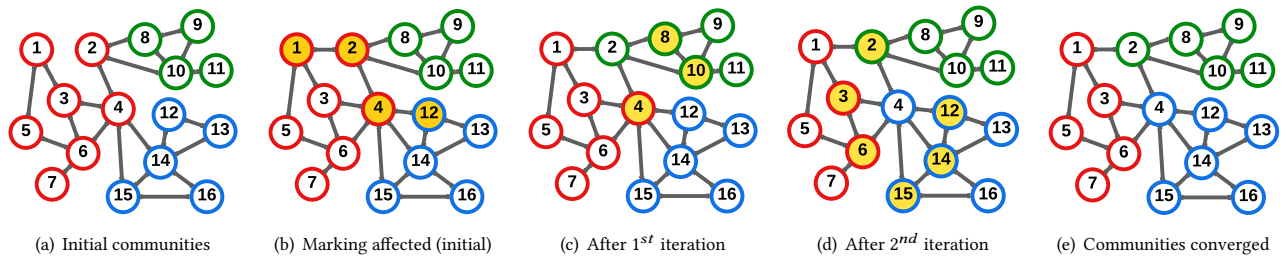


Figure 2: An example explaining our Dynamic Frontier (DF) approach. The community membership of each vertex is shown with border color (red, green, or blue), and the algorithm proceeds from left to right. A batch update arrives, affecting vertices 1, 2, 4, and 12. In the first iteration, vertex 2 switches from red to green, impacting neighbors 8 and 10. In the second iteration, vertex 4 changes from red to blue, affecting neighbors 3, 6, 12, 14, and 15. Afterward, there are no more community changes.

Incremental marking of affected vertices on vertex migration to another community. When a vertex i changes its community during the community detection algorithm (shown by moving i from its original community in the center to its new community on the right), we mark all its neighbor vertices $j \in J_i$ as affected, as shown in Figure 1(c) (highlighted in yellow), and mark i as not affected. To minimize unnecessary computation, we also mark an affected vertex i as not affected even if i does not change its community. We call this as the vertex pruning optimization [44, 55, 59, 74]. The process is akin to a graph traversal and continues until the community assignments of the vertices have converged.

Application to the first pass of Louvain algorithm. We apply the DF approach to the first pass of Louvain algorithm, as with the DS approach. In subsequent passes all super-vertices are marked as affected and processed according to Louvain. This takes less than 14% of total time, so we don't use the DF approach to find affected super-vertices. The pseudocode for our parallel DF Louvain is given in Algorithm 1, with its explanation in Section 4.3. Similar to our parallel ND/DS Louvain, it utilizes auxiliary information.

4.1.1 *An example of DF approach.* See Figure 2.

Initial communities. The original graph consists of 16 vertices, which are divided into three communities, distinguished by the border colors of red, green, and blue (see Figure 2(a)). This community membership of each vertex could have been obtained by executing either the static or dynamic version of Louvain algorithm.

Batch update and marking affected (initial). Subsequently a batch update is applied to the original graph (see Figure 2(b)), involving edge deletion between vertices 1 and 2, and an insertion vertices 4 and 12. Following the batch update, we perform the initial step of the DF approach, marking endpoints 1, 2, 4, and 12 as affected. Now, we are ready to execute the first iteration of Louvain algorithm.

After first iteration. During the first iteration (see Figure 2(c)), the community membership of vertex 2 changes from red to green because it exhibits stronger connections with vertices in the green community. In response to this change, the DF approach incrementally marks the neighboring vertices of 2 as affected, specifically vertices 8 and 10. Vertex 2 is no longer affected due to pruning.

After second iteration. Let us now consider the second iteration (see Figure 2(d)). Vertex 4 is now more strongly connected to the *blue* community, resulting in a change of its community membership from *red* to *blue*. As before, we mark the neighbors of vertex 4 as affected, namely vertices 12, 14, and 15. Vertex 4, once again, no longer marked as affected due to vertex pruning.

Communities converged. In the subsequent iteration (see Figure 2(e)), no other vertices have a strong enough reason to change their community membership. At this point, the aggregation phase commences, consolidating communities into super-vertices to prepare for the subsequent pass of Louvain algorithm.

4.2 Utilizing Auxiliary information

We note that computing the weighted-degree of each vertex K^t and the total edge weight of each community Σ^t incurs considerable runtime, in comparison to the time required for the local-moving and aggregation phases of the Louvain algorithm. It would be more efficient to incrementally update the previous weighted-degrees of vertices K^{t-1} and total edge weights of communities Σ^{t-1} by taking into account edge deletions Δ^{t-} and insertions Δ^{t+} within the batch update, instead of recomputing from scratch. We refer to K^t and Σ^t (and K^{t-1} , Σ^{t-1}) as auxiliary information as they must be maintained by the dynamic algorithm, but do not represent the output of the algorithm. Figure 3 illustrates this concept.

In Figure 4, we present the mean speedup observed for ND, DS, and DF Louvain when making use of auxiliary information K^{t-1} and Σ^{t-1} , in contrast to the same dynamic algorithm when calculating from scratch. This is done on graphs from Table 3 with random batch updates of size $10^{-7}|E|$ to $0.1|E|$, consisting of 80% edge insertions and 20% edge deletions, to simulate realistic dynamic graph updates. Results indicate that employing auxiliary information enables ND, DS, and DF Louvain to achieve average speedups of 11.8 \times , 2.9 \times , and 48.5 \times , respectively. Moreover, DF Louvain achieves remarkable speedups, reaching up to 107 \times for smaller batch sizes. Incrementally updating K^{t-1} and Σ^{t-1} to obtain K^t and Σ^t , thus, significantly speeds up DF Louvain. To the best of our knowledge, none of the existing dynamic algorithms for Louvain algorithm make such use of auxiliary information.

4.3 Our DF Louvain implementation

Algorithm 1 shows the pseudocode of our Parallel Dynamic Frontier (DF) Louvain. It takes as input the previous G^{t-1} and current graph snapshot G^t , edge deletions Δ^{t-} and insertions Δ^{t+} in the batch update, the previous community assignments C^{t-1} for each vertex, the previous weighted-degrees K^{t-1} of vertices, and the previous total edge weights Σ^{t-1} of communities. It returns the updated community memberships C^t of vertices, weighted-degrees K^t , and total edge weights Σ^t of communities.

In the algorithm, we first identify an initial set of affected vertices, whose communities may directly change due to the batch updates, by marking them in the flag vector δV . We do this by marking the endpoints of edge deletions Δ^{t-} which lie in the same community (lines 3-4), and by marking the endpoints of edge insertions Δ^{t+} which lie in disjoint communities (lines 5-6). We then define three lambda functions for the Louvain algorithm, `isAffected()` (lines

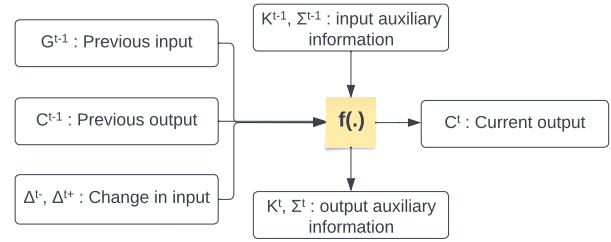


Figure 3: A dynamic community detection algorithm $f(\cdot)$ accepts as input the previous graph G^{t-1} , community memberships C^{t-1} , and the batch update Δ^{t-} , Δ^{t+} , and returns the updated community memberships C^t . However, it may also accept weighted degree of vertices K^{t-1} and total edge weights of communities Σ^{t-1} as auxiliary information, and generate updated auxiliary information K^t , Σ^t .

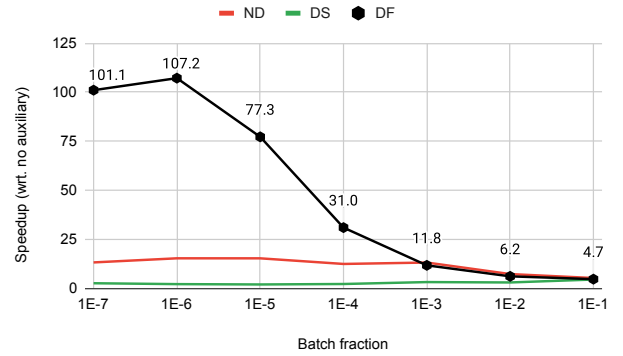


Figure 4: Speedup of Naive-dynamic (ND), Delta-screening (DS), and Dynamic Frontier (DF) Louvain when reusing the previous weighted-degrees of vertices and total edge weight of communities as auxiliary information to the dynamic algorithm, compared to the same dynamic algorithm when both are recomputed from scratch. This is done on large graphs with generated random batch updates of size $10^{-7}|E|$ to $0.1|E|$.

7-8), `inAffectedRange()` (lines 9-10), and `onChange()` (lines 11-12), which indicate that a set of vertices are (initially) marked as affected, that all vertices in the graph can be incrementally marked as affected, and that the neighbors of a vertex are marked as affected if it changes its community membership, respectively. Note that the set of affected vertices will expand automatically due to vertex pruning optimization used in our Parallel Louvain algorithm (Algorithm 4). Thus, `onChange()` reflects what the DF approach would do in the absence of vertex pruning. Further, unlike existing approaches, we leverage K^{t-1} and Σ^{t-1} , alongside the batch updates Δ^{t-} and Δ^{t+} , to efficiently compute K^t and Σ^t required for the local-moving phase of the Louvain algorithm (line 15). These lambda functions and the total vertex/edge weights are then utilized to execute the Louvain algorithm and obtain the updated community assignments C^t (line 17). Finally, we return C^t , alongside K^t and Σ^t (line 18).

Algorithm 1 Our Parallel *Dynamic Frontier (DF)* Louvain.

▷ G^{t-1}, G^t : Previous, current input graph
 ▷ Δ^{t-}, Δ^{t+} : Edge deletions and insertions (batch update)
 ▷ C^{t-1}, C^t : Previous, current community of each vertex
 ▷ K^{t-1}, K^t : Previous, current weighted-degree of vertices
 ▷ Σ^{t-1}, Σ^t : Previous, current total edge weight of communities
 □ δV : Flag vector indicating if each vertex is affected
 □ $isAffected(i)$: Is vertex i marked as affected?
 □ $inAffectedRange(i)$: Can i be incrementally marked?
 □ $onChange(i)$: What happens if i changes its community?
 □ F : Lambda functions passed to parallel Louvain (Alg. 4)

```

1: function DYNAMICFRONTIER( $G^{t-1}, G^t, \Delta^{t-}, \Delta^{t+}, C^{t-1}, K^{t-1}, \Sigma^{t-1}$ )
2:   ▷ Mark initial affected vertices
3:   for all  $(i, j) \in \Delta^{t-}$  in parallel do
4:     if  $C^{t-1}[i] = C^{t-1}[j]$  then  $\delta V[i] \leftarrow 1$ 
5:   for all  $(i, j, w) \in \Delta^{t+}$  in parallel do
6:     if  $C^{t-1}[i] \neq C^{t-1}[j]$  then  $\delta V[i] \leftarrow 1$ 
7:   function ISAFFECTED( $i$ )
8:     return  $\delta V[i]$ 
9:   function INAFFECTEDRANGE( $i$ )
10:    return 1
11:  function ONCHANGE( $i$ )
12:    for all  $j \in G^t.neighbors(i)$  do  $\delta V[j] \leftarrow 1$ 
13:   $F \leftarrow \{isAffected, inAffectedRange, onChange\}$ 
14:  ▷ Use  $K^{t-1}, \Sigma^{t-1}$  as auxiliary information (Alg. 7)
15:   $\{K^t, \Sigma^t\} \leftarrow updateWeights(G^t, \Delta^{t-}, \Delta^{t+}, C^{t-1}, K^{t-1}, \Sigma^{t-1})$ 
16:  ▷ Obtain updated communities (Alg. 4)
17:   $C^t \leftarrow louvain(G^t, C^{t-1}, K^t, \Sigma^t, F)$ 
18:  return  $\{C^t, K^t, \Sigma^t\}$ 
  
```

5 EVALUATION

5.1 Experimental setup

5.1.1 System. For our experiments, we use a server that has an x86-based 64-bit AMD EPYC-7742 processor. This processor has a clock frequency of 2.25 GHz and 512 GB of DDR4 system memory. Each core has an L1 cache of 4 MB, an L2 cache of 32 MB, and a shared L3 cache of 256 MB. The machine uses Ubuntu 20.04.

5.1.2 Configuration. We use 32-bit unsigned integer for vertex IDs, 32-bit floating point for edge weights, but use 64-bit floating point for hashtable values, total edge weight, modularity calculation, and all places where performing an aggregation/sum of floating point values. Affected vertices are represented with an 8-bit integer vector. Computing the weighted degree of each vertex, the local moving phase, and aggregating the edges for the super-vertex graph, employ OpenMP’s *dynamic schedule* with a chunk size of 2048 for dynamic workload balancing among threads. We set the iteration tolerance τ to 10^{-2} , the tolerance drop per pass *TOLERANCE_DECLINE_FACTOR* to 10 (threshold-scaling optimization), maximum number of iterations per pass *MAX_ITERATIONS* to 20, and the maximum number of passes *MAX_PASSES* to 10. Further, we set the aggregation tolerance τ_{agg} to 0.8 for large (static) graphs with generated random batch updates, but keep it

disabled, i.e., set τ_{agg} to 1, for real-world dynamic graphs. Unless mentioned otherwise, we execute all parallel implementations with a default of 64 threads (to match the number of cores available on the system). We use GCC 9.4 and OpenMP 5.0 [43] for compilation.

5.1.3 Dataset. To experiment with real-world dynamic graphs, we employ five temporal networks sourced from the Stanford Large Network Dataset Collection [33], detailed in Table 2. Here, the number of vertices range from 24.8 thousand to 2.60 million, temporal edges from 507 thousand to 63.4 million, and static edges from 240 thousand to 36.2 million. For experiments involving large static graphs with random batch updates, we utilize 12 graphs as listed in Table 3, obtained from the SuiteSparse Matrix Collection [30]. Here, the number of vertices in the graphs varies from 3.07 to 214 million, and the number of edges varies from 25.4 million to 3.80 billion. With each graph, we ensure that all edges are undirected and weighted with a default weight of 1.

Table 2: List of 5 real-world dynamic graphs, sourced from the Stanford Large Network Dataset Collection [33]. Here, $|V|$ denotes the number of vertices, $|E_T|$ represents the count of temporal edges (inclusive of duplicates), and $|E|$ indicates the number of static edges (without duplicates).

Graph	$ V $	$ E_T $	$ E $
sx-mathoverflow	24.8K	507K	240K
sx-askubuntu	159K	964K	597K
sx-superuser	194K	1.44M	925K
wiki-talk-temporal	1.14M	7.83M	3.31M
sx-stackoverflow	2.60M	63.4M	36.2M

5.1.4 Batch generation. For experiments involving real-world dynamic graphs, we first load 90% of each graph from Table 2, and ensure that all edges are weighted with a default weight of 1, and that they are undirected by adding the reverse edges. Subsequently, we load B edges in 100 batch updates. Here, B denotes the desired batch size, specified as a fraction of the total number of temporal edges $|E_T|$ in the graph, and ensure that the batch update is undirected. For experiments on large graphs with random batch updates, we take each base graph from Table 3 and generate random batch updates [72] comprising an 80% : 20% mix of edge insertions and deletions to emulate realistic batch updates, each with an edge weight of 1. To prepare the set of edges for insertion, we select vertex pairs with equal probability. For edge deletions, we uniformly delete each existing edge. To simplify, we ensure no new vertices are added or removed from the graph. The batch size is measured as a fraction of edges in the original graph, ranging from 10^{-7} to 0.1 (i.e., $10^{-7}|E|$ to $0.1|E|$), with multiple batches generated for each size for averaging. For a billion-edge graph, this amounts to a batch size of 100 to 100 million edges. All batch updates are undirected, i.e., for every edge insertion (i, j, w) in the batch update, the edge (j, i, w) is also a part of the batch update. We employ five distinct random batch updates for each batch size, and report average across these runs in our experiments.

Table 3: List of 12 graphs obtained from the SuiteSparse Matrix Collection [30] (directed graphs are marked with *). Here, $|V|$ is the total number of vertices, $|E|$ is the total number of edges (after making the graph undirected), and $|\Gamma|$ is the number of communities obtained using *Static Louvain* [56].

Graph	$ V $	$ E $	$ \Gamma $
Web Graphs (LAW)			
indochina-2004*	7.41M	341M	4.24K
arabic-2005*	22.7M	1.21B	3.66K
uk-2005*	39.5M	1.73B	20.8K
webbase-2001*	118M	1.89B	2.76M
it-2004*	41.3M	2.19B	5.28K
sk-2005*	50.6M	3.80B	3.47K
Social Networks (SNAP)			
com-LiveJournal	4.00M	69.4M	2.54K
com-Orkut	3.07M	234M	29
Road Networks (DIMACS10)			
asia_osm	12.0M	25.4M	2.38K
europa_osm	50.9M	108M	3.05K
Protein k-mer Graphs (GenBank)			
kmer_A2a	171M	361M	21.2K
kmer_V1r	214M	465M	6.17K

5.1.5 Measurement. We evaluate the runtime of each approach on the entire updated graph, including the local-moving phase, aggregation phase, the initial and incremental marking of affected vertices, convergence detection, and all the necessary intermediary steps, but excluding memory allocation/deallocation time. We assume that the total edge weight of the graphs is known, and can be tracked upon each batch update.

5.2 Performance Comparison

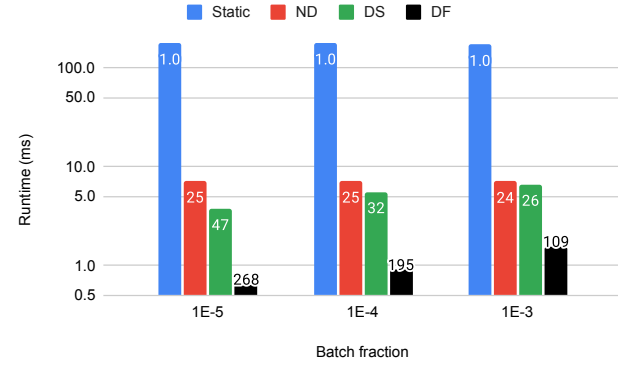
5.2.1 Results on real-world dynamic graphs. We now compare the performance of our Parallel Dynamic Frontier (DF) Louvain with our parallel implementation of Static, Naive-dynamic (ND), and Delta-screening (DS) Louvain on real-world dynamic graphs from Table 2. These evaluations are conducted on batch updates of size $10^{-5}|E_T|$ to $10^{-3}|E_T|$ in multiples of 10. For each batch size, as mentioned in Section 5.1.4, we load 90% of the graph, add reverse edges to make all edges in the graph undirected, and then load B edges (where B is the batch size) consecutively in 100 batch updates. The work of Zarayeneh et al. [72] demonstrates improved performance of the DS approach compared to DynaMo [75] and Batch [11]. Thus, we limit our comparison to DS Louvain. Figure 5(a) displays the overall runtime of each approach across all graphs for each batch size, while Figure 5(b) illustrates the overall modularity of obtained communities. Additionally, Figures 5(c) and 5(d) present the mean runtime and modularity of communities obtained with the approaches on each dynamic graph in the dataset. Finally, Figures 11, 12, 13, 14, and 15 show the runtime and modularity of communities obtained with Static, ND, DS, and DF Louvain on each dynamic graph in Table 2, upon each consecutive batch update.

Figure 5(a) shows that DF Louvain is, on average, 268 \times , 195 \times , and 109 \times faster than Static Louvain on batch updates of size $10^{-5}|E_T|$, $10^{-4}|E_T|$, and $10^{-3}|E_T|$, respectively. In contrast, DS Louvain demonstrates average speedups of 47 \times , 32 \times , and 26 \times over Static Louvain for batch update sizes of $10^{-5}|E_T|$ to $10^{-3}|E_T|$, while ND Louvain obtains a mean speedup of 25 \times . DF Louvain is thus, overall, 179 \times , 7.2 \times , and 5.3 \times faster than Static, ND, and DS Louvain. This speedup is particularly pronounced on the *sx-superuser* graph, as indicated by Figure 5(c). Regarding modularity, Figures 5(b) and 5(d) illustrate that DF Louvain generally exhibits slightly lower modularity on average compared to ND and DS Louvain but is on par with the modularity obtained by Static Louvain, except for the *sx-superuser* graph (because it fails to mark certain vertices as affected, likely because they are outlier vertices and were not directly reached from the expanding frontier). This makes the communities obtained with DF Louvain generally acceptable. However, if lower modularity is observed (during intermediate empirical tests), transitioning to our parallel implementation of DS Louvain is advisable.

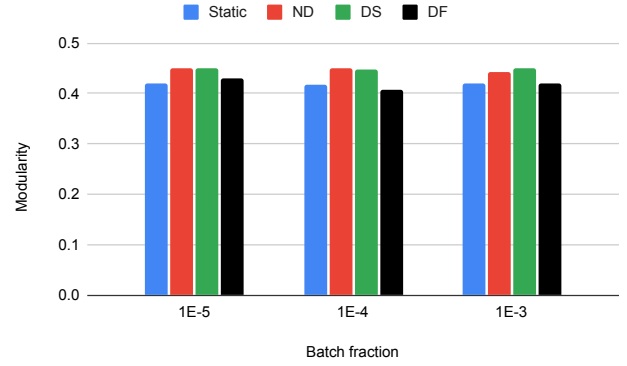
5.2.2 Results on large graphs with random batch updates. We also assess the performance of our parallel DF Louvain alongside our parallel implementation of Static, ND, and DS Louvain on large (static) graphs listed in Table 3, with randomly generated batch updates. As elaborated in Section 5.1.4, the batch updates vary in size from $10^{-7}|E|$ to $0.1|E|$ (in multiples of 10), comprising 80% edge insertions and 20% edge deletions to mimic realistic scenarios. Reverse edges are added with each batch update, to ensure that the graph is undirected. As mentioned in Section 5.1.4, we generate 5 different random batch updates for each batch size to minimize measurement noise. Figure 6 illustrates the runtime of Static, ND, DS, and DF Louvain, while Figure 7 displays the modularity of communities obtained with each approach.

Figure 6(a) illustrates that DF Louvain achieves a mean speedup of 183 \times , 13.8 \times , and 8.7 \times compared to Static, ND, and DS Louvain, respectively. On a batch update of size $10^{-7}|E|$, DF Louvain is significantly faster, attaining speedups of 540 \times , 39 \times , and 14 \times , with respect to Static, ND, and DS Louvain, respectively. The speedup is particularly pronounced on web graphs, social networks, and protein k-mer graphs, characterized by a large number of vertices (as depicted in Figure 6(b)). It may be noted that DS Louvain exhibits slower performance than ND Louvain on large batch updates, i.e., on batch updates of size $0.01|E|$ and $0.1|E|$. This is attributed to the cost of initial marking of affected vertices with DS Louvain — since the updates are scattered randomly across the graph, DS Louvain ends up marking a significant number of vertices as affected, making it almost equivalent to ND Louvain, but with the added cost of the marking of affected vertices (particularly on web graphs and social networks, characterized by a high average degree and a small diameter). Figures 7(a) and 7(b) indicate that DF Louvain obtains communities with the roughly same modularity as Static, ND, and DS Louvain. Hence, for large graphs with random batch updates, DF Louvain is the best dynamic community detection method.

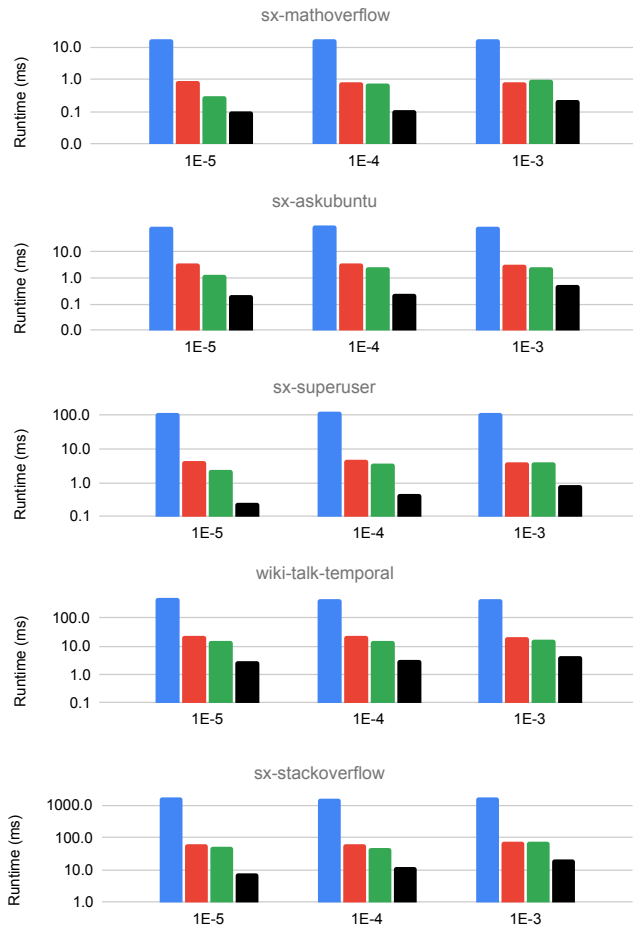
In Figure 6, also note that runtime of Static Louvain increases for larger batch updates. This more likely due to the random batch updates arbitrarily disrupting the original community structure — which results in Static Louvain needing more iterations to converge — than due to the increased number of edges in the graph.



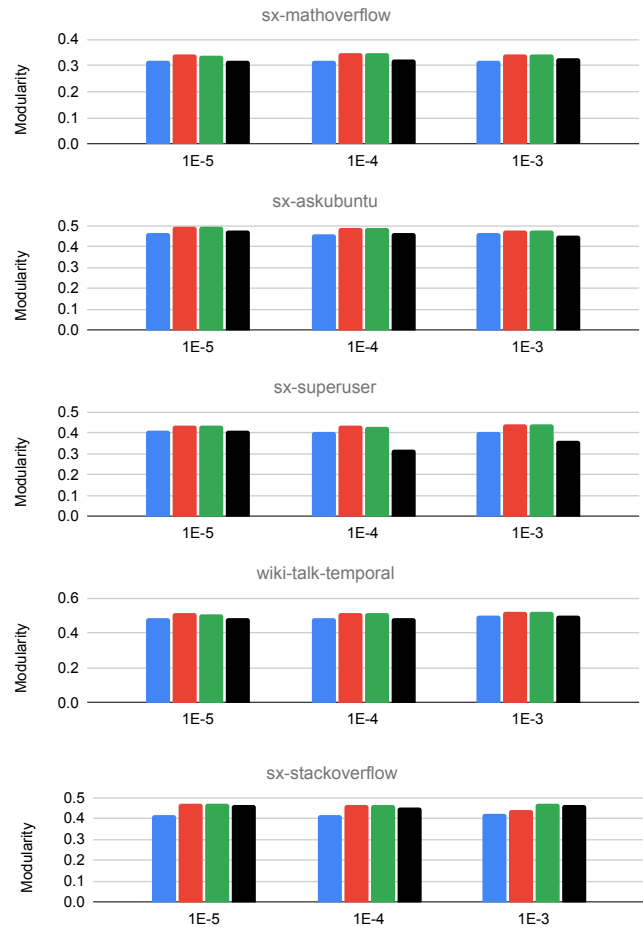
(a) Overall Runtime



(b) Overall Modularity of communities obtained



(c) Runtime on each dynamic graph



(d) Modularity in communities obtained on each dynamic graph

Figure 5: Mean Runtime and Modularity of communities obtained with our multicore implementation of *Static*, *Naive-dynamic (ND)*, *Delta-screening (DS)*, and *Dynamic Frontier (DF)* PageRank on real-world dynamic graphs, with batch updates of size $10^{-5}|E_T|$ to $10^{-3}|E_T|$. Here, (a) and (b) show the overall runtime and modularity across all temporal graphs, while (c) and (d) show the runtime and modularity for each graph. In (a), the speedup of each approach with respect to Static Louvain is labeled.

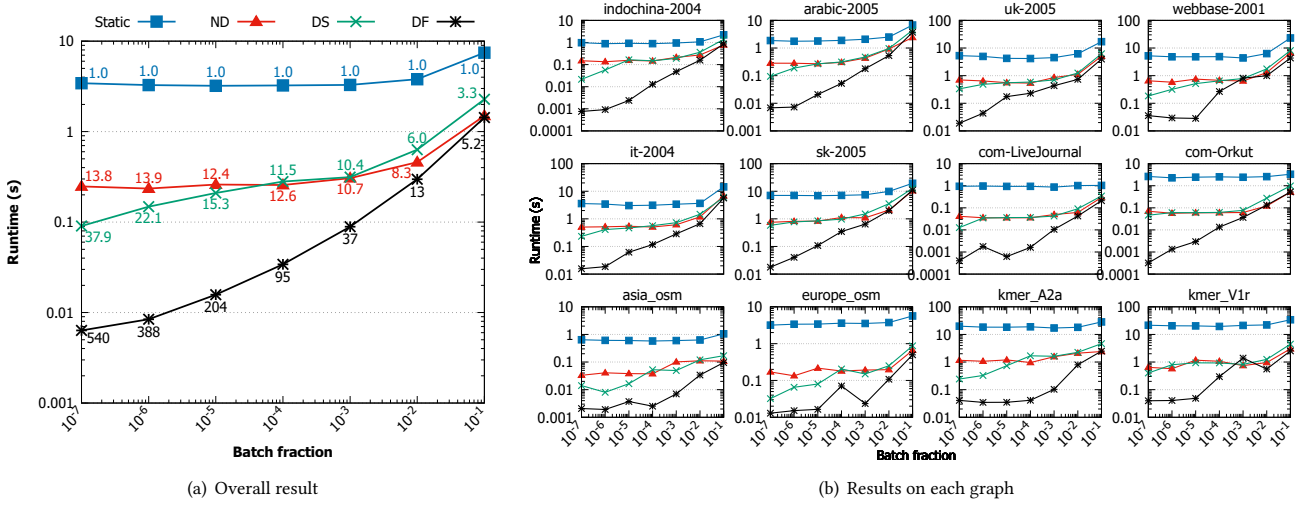


Figure 6: Runtime (logarithmic scale) of our multicore implementation of *Static*, *Naive-dynamic (ND)*, *Delta-screening (DS)*, and *Dynamic Frontier (DF)* Louvain on large (static) graphs with generated random batch updates. Batch updates range in size from $10^{-7}|E|$ to $0.1|E|$ in multiples of 10. These updates consist of 80% edge insertions and 20% edge deletions, mimicking realistic changes in a dynamic graph scenario. The right subfigure illustrates the runtime of each approach for individual graphs in the dataset, while the left subfigure presents overall runtimes (using geometric mean for consistent scaling across graphs). Additionally, the speedup of each approach relative to *Static* Louvain is labeled on respective lines.

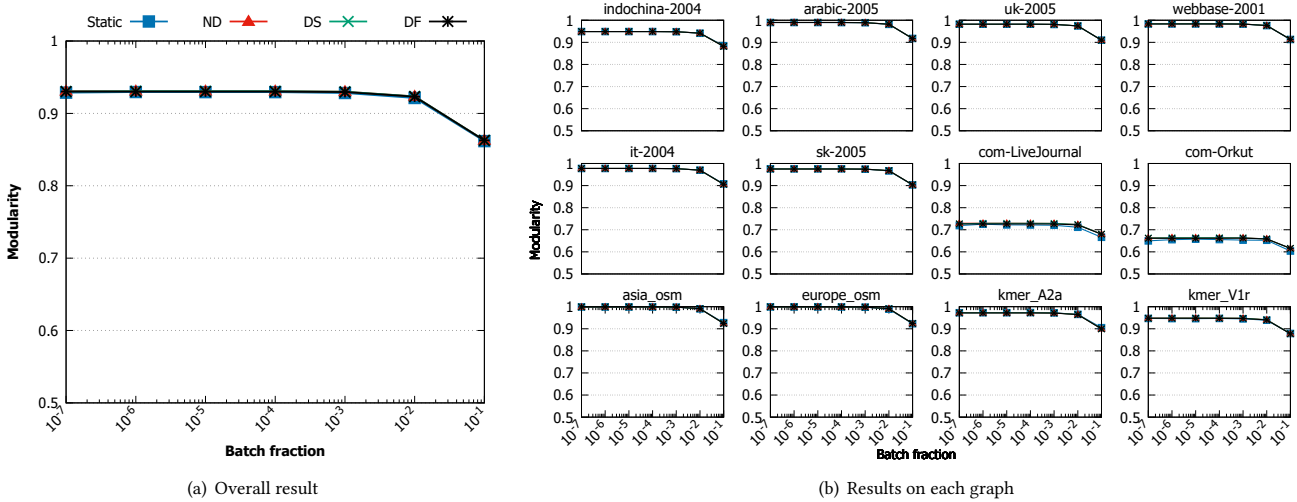
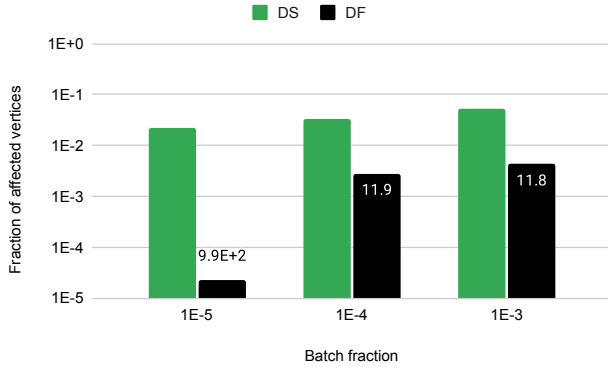


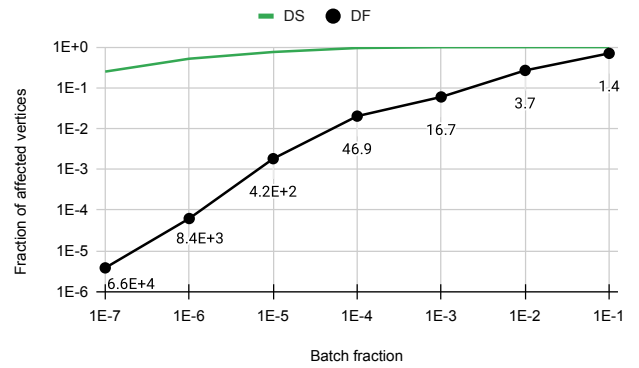
Figure 7: Modularity comparison of our multicore implementation of *Static*, *Naive-dynamic (ND)*, *Delta-screening (DS)*, and *Dynamic Frontier (DF)* Louvain on large (static) graphs with generated random batch updates. The size of batch updates range from $10^{-7}|E|$ to $0.1|E|$ in multiples of 10 (logarithmic scale), consisting of 80% edge insertions and 20% edge deletions to simulate realistic dynamic graph updates. The right subfigure depicts the modularity for each approach in relation to each graph, while the left subfigure showcases overall modularity using arithmetic mean.

5.2.3 *Comparison of vertices marked as affected.* Figure 8(a) displays the mean percentage of vertices marked as affected by DS and DF Louvain on real-world dynamic graphs from Table 2, with batch updates of size $10^{-5}|E_T|$ to $10^{-3}|E_T|$ in multiples of 10 (see Section 5.1.4 for details) – while Figure 8(b) displays the mean percentage of vertices marked as affected by DS and DF Louvain on large

(static) graphs with generated random batch updates (consisting of 80% edge insertions and 20% deletions), on batch updates of size $10^{-7}|E|$ to $0.1|E|$. For DS Louvain, the affected vertices are marked at the start of the algorithm, while, for DF Louvain, affected vertices are marked incrementally – therefore, we count all vertices that were ever flagged as affected with DF Louvain.



(a) Mean percentage of affected vertices on real-world dynamic graphs



(b) Mean percentage of affected vertices on large graphs with random batch updates

Figure 8: Mean percentage of vertices marked as affected by *Delta-screening (DS)* and our *Dynamic Frontier (DF)* Louvain, on real-world dynamic graphs (with batch updates of size $10^{-5}|E|$ to $10^{-3}|E|$), and on large graphs with random batch updates (80% edge insertions and 20% edge deletions with batch updates of size $10^{-7}|E|$ to $0.1|E|$).

Figure 8(a) shows that the proportion of vertices marked as affected by DF Louvain is 990 \times , 11.9 \times , and 11.8 \times lower than DS Louvain for batch updates of size $10^{-5}|E|$, $10^{-4}|E|$, and $10^{-3}|E|$, respectively. Figure 8(b) also paints a similar picture, with significantly fewer vertices being marked as affected by DF Louvain for smaller batch updates (i.e., batch updates of size $10^{-7}|E|$ and $10^{-6}|E|$). Therefore, the performance improvement with DF Louvain can be attributed to both marking fewer vertices as affected, and to the incremental marking of affected vertices. Additionally, it is worth noting that, on real-world dynamic graphs, the fraction of vertices marked as affected is generally low across both approaches. This is likely because updates in such graphs tend to be concentrated in specific regions of the graph.

5.2.4 Strong scaling. Finally, we study the strong-scaling behavior of DF Louvain on large (static) graphs, with generated random batch updates of size $10^{-7}|E|$ to $0.1|E|$. The speedup of DF Louvain is measured as the number of threads increases from 1 to 64 in multiples of 2, relative to single-threaded execution. This process is repeated for each graph in the dataset (refer to Table 2), and the results are averaged using geometric mean.

The results, depicted in Figure 9, indicate that with 16 threads, DF Louvain achieves an average speedup of 6.6 \times compared to single-threaded execution, showing a performance increase of 1.6 \times for every doubling of threads. The speedup of DF Louvain is lower, likely due to the reduced work performed by the algorithm. At 32 and 64 threads, DF Louvain is affected by NUMA effects (the 64-core processor used has 4 NUMA domains), resulting in a speedup of only 6.9 \times and 6.5 \times , respectively. The results are similar on real-world dynamic graphs, but the speedup is even lower for 64 threads due to lack of sufficient work per thread.

6 CONCLUSION

In conclusion, in this report we presented our Parallel Dynamic Frontier (DF) Louvain algorithm, which given a batch update of edge deletions or insertions, incrementally identifies and processes

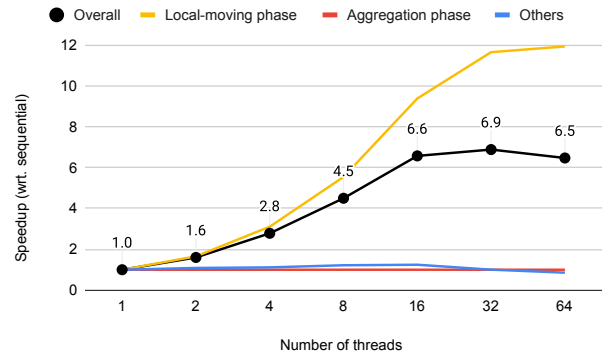


Figure 9: Mean speedup of *Dynamic Frontier (DF)* Louvain with increasing number of threads (in multiples of 2), on large graphs with random batch updates of size $10^{-7}|E|$ to $0.1|E|$, composed 80% edge insertions and 20% insertions.

an approximate set of affected vertices in the graph with minimal overhead. In addition, we use a novel approach of incrementally updating weighted-degrees of vertices and total edge weights of communities, by using them as auxiliary information to DF Louvain. We also present our parallel implementations of Naive-dynamic (ND) [3] and Delta-screening (DS) Louvain [72]. On a server with a 64-core AMD EPYC-7742 processor, our experiments show that DF Louvain obtains speedups of 179 \times , 7.2 \times , and 5.3 \times on real-world dynamic graphs, compared to Static, ND, and DS Louvain, respectively, and is 183 \times , 13.8 \times , and 8.7 \times faster, respectively, on large graphs with random batch updates. The performance of DF Louvain can be attributed to incremental marking, and marking of fewer vertices. Furthermore, DF Louvain improves performance at a rate of 1.6 \times for every doubling of threads. DF Louvain is based on one of the fastest implementations of Static Louvain [56] and thus offers state-of-the-art performance. However, we observe DF Louvain to

obtain lower modularity score on the *sx-superuser* real-world dynamic graph. We thus recommend the reader to use DF Louvain for updating community memberships on dynamic graphs, but switch to DS Louvain if lower modularity is observed.

ACKNOWLEDGMENTS

I would like to thank Prof. Kishore Kothapalli and Prof. Dip Sankar Banerjee for their support.

REFERENCES

- [1] R. Aktunc, I. Toroslu, M. Ozer, and H. Davulcu. 2015. A dynamic modularity based community detection algorithm for large-scale networks: DSLM. In *Proceedings of the IEEE/ACM international conference on advances in social networks analysis and mining*, 1177–1183.
- [2] A. Aldabobi, A. Shariéh, and R. Jabri. 2022. An improved Louvain algorithm based on Node importance for Community detection. *Journal of Theoretical and Applied Information Technology* 100, 23 (2022), 1–14.
- [3] T. Aynaud and J. Guillaume. 2010. Static community detection algorithms for evolving networks. In *8th International Symposium on Modeling and Optimization in Mobile, Ad Hoc, and Wireless Networks*. IEEE, IEEE, Avignon, France, 513–519.
- [4] Thomas Aynaud and Jean-Loup Guillaume. 2011. Multi-step community detection and hierarchical time segmentation in evolving networks. In *Proceedings of the 5th SNA-KDD workshop*, Vol. 11.
- [5] A. Bhowmick, S. Vadhiyar, and V. PV. 2022. Scalable multi-node multi-GPU Louvain community detection algorithm for heterogeneous architectures. *Concurrency and Computation: Practice and Experience* 34, 17 (2022), 1–18.
- [6] A. Bhowmik and S. Vadhiyar. 2019. HyDetect: A Hybrid CPU-GPU Algorithm for Community Detection. In *IEEE 26th International Conference on High Performance Computing, Data, and Analytics (HiPC)*. IEEE, IEEE, Goa, India, 2–11.
- [7] V. Blondel, J. Guillaume, R. Lambiotte, and E. Lefebvre. 2008. Fast unfolding of communities in large networks. *Journal of Statistical Mechanics: Theory and Experiment* 2008, 10 (Oct 2008), P10008.
- [8] U. Brandes, D. Delling, M. Gaertler, R. Gorke, M. Hoefer, Z. Nikoloski, and D. Wagner. 2007. On modularity clustering. *IEEE transactions on knowledge and data engineering* 20, 2 (2007), 172–188.
- [9] C. Cheong, H. Huynh, D. Lo, and R. Goh. 2013. Hierarchical Parallel Algorithm for Modularity-Based Community Detection Using GPUs. In *Proceedings of the 19th International Conference on Parallel Processing (Aachen, Germany) (Euro-Par’13)*. Springer-Verlag, Berlin, Heidelberg, 775–787.
- [10] Yun Chi, Xiaodan Song, Dengyong Zhou, Koji Hino, and Belle L Tseng. 2009. On evolutionary spectral clustering. *ACM Transactions on Knowledge Discovery from Data (TKDD)* 3, 4 (2009), 1–30.
- [11] W. Chong and L. Teow. 2013. An incremental batch technique for community detection. In *Proceedings of the 16th International Conference on Information Fusion*. IEEE, IEEE, Istanbul, Turkey, 750–757.
- [12] Han-Yi Chou and Sayan Ghosh. 2022. Batched Graph Community Detection on GPUs. In *Proceedings of the International Conference on Parallel Architectures and Compilation Techniques*. 172–184.
- [13] M. Cordeiro, R. Sarmento, and J. Gama. 2016. Dynamic community detection in evolving networks using locality modularity optimization. *Social Network Analysis and Mining* 6, 1 (2016), 1–20.
- [14] E. Côme and P. Latouche. 2015. Model selection and clustering in stochastic block models based on the exact integrated complete data likelihood. *Statistical Modelling* 15 (3 2015), 564–589. Issue 6. <https://doi.org/10.1177/1471082X15577017> doi: 10.1177/1471082X15577017.
- [15] I. Derényi, G. Palla, and T. Vicsek. 2005. Clique percolation in random networks. *Physical review letters* 94, 16 (2005), 160202.
- [16] M. Fazlali, E. Moradi, and H. Malazi. 2017. Adaptive parallel Louvain community detection on a multicore platform. *Microprocessors and microsystems* 54 (Oct 2017), 26–34.
- [17] S. Fortunato. 2010. Community detection in graphs. *Physics reports* 486, 3-5 (2010), 75–174.
- [18] O. Gach and J. Hao. 2014. Improving the Louvain algorithm for community detection with modularity maximization. In *Artificial Evolution: 11th International Conference, Evolution Artificielle, EA , Bordeaux, France, October 21-23, . Revised Selected Papers 11*. Springer, Springer, Bordeaux, France, 145–156.
- [19] N. Gawande, S. Ghosh, M. Halappanavar, A. Tumeo, and A. Kalyanaraman. 2022. Towards scaling community detection on distributed-memory heterogeneous systems. *Parallel Comput.* 111 (2022), 102898.
- [20] S. Ghosh, M. Halappanavar, A. Tumeo, A. Kalyanaraman, and A.H. Gebremedhin. 2018. Scalable distributed memory community detection using vite. In *2018 IEEE High Performance extreme Computing Conference (HPEC)*. IEEE, 1–7.
- [21] S. Ghosh, M. Halappanavar, A. Tumeo, A. Kalyanaraman, H. Lu, D. Chavarria-Miranda, A. Khan, and A. Gebremedhin. 2018. Distributed louvain algorithm for graph community detection. In *IEEE International Parallel and Distributed Processing Symposium (IPDPS)*. Vancouver, British Columbia, Canada, 885–895.
- [22] A. Ghoshal, N. Das, S. Bhattacharjee, and G. Chakraborty. 2019. A fast parallel genetic algorithm based approach for community detection in large networks. In *11th International Conference on Communication Systems & Networks (COM-SNETS)*. IEEE, Bangalore, India, 95–101.
- [23] S. Gregory. 2010. Finding overlapping communities in networks by label propagation. *New Journal of Physics* 12 (10 2010), 103018. Issue 10.
- [24] R. Guimera and L. Amaral. 2005. Functional cartography of complex metabolic networks. *nature* 433, 7028 (2005), 895–900.
- [25] S. Gupta, D. Singh, and J. Choudhary. 2022. A review of clique-based overlapping community detection algorithms. *Knowledge and Information Systems* 64, 8 (2022), 2023–2058.
- [26] M. Halappanavar, H. Lu, A. Kalyanaraman, and A. Tumeo. 2017. Scalable static and dynamic community detection using Grappolo. In *IEEE High Performance Extreme Computing Conference (HPEC)*. IEEE, Waltham, MA USA, 1–6.
- [27] P. Held, B. Krause, and R. Kruse. 2016. Dynamic clustering in social networks using louvain and infomap method. In *Third European Network Intelligence Conference (ENIC)*. IEEE, IEEE, Wroclaw, Poland, 61–68.
- [28] Todd Hricik, David Bader, and Oded Green. 2020. Using RAPIDS AI to accelerate graph data science workflows. In *2020 IEEE High Performance Extreme Computing Conference (HPEC)*. IEEE, 1–4.
- [29] K. Kloster and D. Gleich. 2014. Heat kernel based community detection. In *Proceedings of the 20th ACM SIGKDD international conference on Knowledge discovery and data mining*. ACM, New York, USA, 1386–1395.
- [30] S. Kolodziej, M. Aznavah, M. Bullock, J. David, T. Davis, M. Henderson, Y. Hu, and R. Sandstrom. 2019. The SuiteSparse matrix collection website interface. *JOSS* 4, 35 (Mar 2019), 1244.
- [31] A. Lancichinetti and S. Fortunato. 2009. Community detection algorithms: a comparative analysis. *Physical Review E, Statistical, Nonlinear, and Soft Matter Physics* 80, 5 Pt 2 (Nov 2009), 056117.
- [32] J. Leskovec. 2021. CS224W: Machine Learning with Graphs | 2021 | Lecture 13.3 - Louvain Algorithm. <https://www.youtube.com/watch?v=0zuiLBOIcsw>
- [33] Jure Leskovec and Andrej Krevl. 2014. SNAP Datasets: Stanford Large Network Dataset Collection. <http://snap.stanford.edu/data>.
- [34] H. Lu, M. Halappanavar, and A. Kalyanaraman. 2015. Parallel heuristics for scalable community detection. *Parallel computing* 47 (Aug 2015), 19–37.
- [35] Y. Lu and G. Chakraborty. 2020. Improving Efficiency of Graph Clustering by Genetic Algorithm Using Multi-Objective Optimization. *International Journal of Applied Science and Engineering* 17, 2 (Jun 2020), 157–173.
- [36] X. Meng, Y. Tong, X. Liu, S. Zhao, X. Yang, and S. Tan. 2016. A novel dynamic community detection algorithm based on modularity optimization. In *7th IEEE international conference on software engineering and service science (ICSESS)*. IEEE, IEEE, Beijing, China, 72–75.
- [37] M. Mohammadi, M. Fazlali, and M. Hosseinzadeh. 2020. Accelerating Louvain community detection algorithm on graphic processing unit. *The Journal of supercomputing* (Nov 2020).
- [38] M. Naim, F. Manne, M. Halappanavar, and A. Tumeo. 2017. Community detection on the GPU. In *IEEE International Parallel and Distributed Processing Symposium (IPDPS)*. IEEE, Orlando, Florida, USA, 625–634.
- [39] M. Newman. 2004. Detecting community structure in networks. *The European Physical Journal B - Condensed Matter* 38, 2 (Mar 2004), 321–330.
- [40] M. Newman. 2006. Finding community structure in networks using the eigenvectors of matrices. *Physical review E* 74, 3 (2006), 036104.
- [41] M. Newman and G. Reinert. 2016. Estimating the number of communities in a network. *Physical review letters* 117, 7 (2016), 078301.
- [42] Nam P Nguyen, Thang N Dinh, Sindhura Tokala, and My T Thai. 2011. Overlapping communities in dynamic networks: their detection and mobile applications. In *Proceedings of the 17th annual international conference on Mobile computing and networking*. 85–96.
- [43] OpenMP Architecture Review Board. 2018. OpenMP Application Program Interface Version 5.0. <https://www.openmp.org/wp-content/uploads/OpenMP-API-Specification-5.0.pdf>
- [44] N. Ozaki, H. Tezuka, and M. Inaba. 2016. A simple acceleration method for the Louvain algorithm. *International Journal of Computer and Electrical Engineering* 8, 3 (2016), 207.
- [45] Hang Qie, Shijie Li, Yong Dou, Jinwei Xu, Yunsheng Xiong, and Zikai Gao. 2022. Isolate sets partition benefits community detection of parallel Louvain method. *Scientific Reports* 12, 1 (2022), 8248.
- [46] X. Que, F. Checconi, F. Petrini, and J. Gunnels. 2015. Scalable community detection with the louvain algorithm. In *IEEE International Parallel and Distributed Processing Symposium*. IEEE, IEEE, Hyderabad, India, 28–37.
- [47] U. Raghavan, R. Albert, and S. Kumara. 2007. Near linear time algorithm to detect community structures in large-scale networks. *Physical Review E* 76, 3 (Sep 2007), 036106–1–036106–11.
- [48] G. Ramalingam. 1996. *Bounded Incremental Computation*. Vol. 1089. Springer-Verlag, LNCS.

- [49] J. Reichardt and S. Bornholdt. 2006. Statistical mechanics of community detection. *Physical review E* 74, 1 (2006), 016110.
- [50] L. Rita. 2020. Infomap Algorithm. An algorithm for community finding. <https://towardsdatascience.com/infomap-algorithm-9b68b7e8b86>
- [51] M. Rosvall, D. Axelsson, and C. Bergstrom. 2009. The map equation. *The European Physical Journal Special Topics* 178, 1 (Nov 2009), 13–23.
- [52] M. Rosvall and C. Bergstrom. 2008. Maps of random walks on complex networks reveal community structure. *Proceedings of the national academy of sciences* 105, 4 (2008), 1118–1123.
- [53] R. Rotta and A. Noack. 2011. Multilevel local search algorithms for modularity clustering. *Journal of Experimental Algorithmics (JEA)* 16 (2011), 2–1.
- [54] Y. Ruan, D. Fuhry, J. Liang, Y. Wang, and S. Parthasarathy. 2015. *Community discovery: simple and scalable approaches*. Springer International Publishing, Cham, 23–54.
- [55] S. Ryu and D. Kim. 2016. Quick community detection of big graph data using modified louvain algorithm. In *IEEE 18th International Conference on High Performance Computing and Communications (HPCC)*. IEEE, Sydney, NSW, 1442–1445.
- [56] Subhajit Sahu. 2023. GVE-Louvain: Fast Louvain Algorithm for Community Detection in Shared Memory Setting. *arXiv preprint arXiv:2312.04876* (2023).
- [57] Naw Safrin Sattar and Shaikh Arifuzzaman. 2022. Scalable distributed Louvain algorithm for community detection in large graphs. *The Journal of Supercomputing* 78, 7 (2022), 10275–10309.
- [58] J. Shang, L. Liu, F. Xie, Z. Chen, J. Miao, X. Fang, and C. Wu. 2014. A real-time detecting algorithm for tracking community structure of dynamic networks.
- [59] J. Shi, L. Dhulipala, D. Eisenstat, J. Łącki, and V. Mirrokni. 2021. Scalable community detection via parallel correlation clustering.
- [60] C.L. Staudt, A. Sazonovs, and H. Meyerhenke. 2016. NetworKit: A tool suite for large-scale complex network analysis. *Network Science* 4, 4 (2016), 508–530.
- [61] Christian L Staudt and Henning Meyerhenke. 2015. Engineering parallel algorithms for community detection in massive networks. *IEEE Transactions on Parallel and Distributed Systems* 27, 1 (2015), 171–184.
- [62] V. Traag. 2015. Faster unfolding of communities: Speeding up the Louvain algorithm. *Physical Review E* 92, 3 (2015), 032801.
- [63] V. Traag, P. Dooren, and Y. Nesterov. 2011. Narrow scope for resolution-limit-free community detection. *Physical Review E* 84, 1 (2011), 016114.
- [64] V. Traag, L. Waltman, and N. Eck. 2019. From Louvain to Leiden: guaranteeing well-connected communities. *Scientific Reports* 9, 1 (Mar 2019), 5233.
- [65] L. Waltman and N. Eck. 2013. A smart local moving algorithm for large-scale modularity-based community detection. *The European physical journal B* 86, 11 (2013), 1–14.
- [66] C. Wickramaarachchi, M. Frincu, P. Small, and V. Prasanna. 2014. Fast parallel algorithm for unfolding of communities in large graphs. In *IEEE High Performance Extreme Computing Conference (HPEC)*. IEEE, IEEE, Waltham, MA USA, 1–6.
- [67] J. Xie, M. Chen, and B. Szymanski. 2013. LabelrankT: Incremental community detection in dynamic networks via label propagation. In *Proceedings of the Workshop on Dynamic Networks Management and Mining*. ACM, New York, USA, 25–32.
- [68] J. Xie, B. Szymanski, and X. Liu. 2011. SLPA: Uncovering overlapping communities in social networks via a speaker-listener interaction dynamic process. In *IEEE 11th International Conference on Data Mining Workshops*. IEEE, IEEE, Vancouver, Canada, 344–349.
- [69] Jierui Xie and Boleslaw K Szymanski. 2013. Labelrank: A stabilized label propagation algorithm for community detection in networks. In *2013 IEEE 2nd Network Science Workshop (NSW)*. IEEE, 138–143.
- [70] S. Yin, S. Chen, Z. Feng, K. Huang, D. He, P. Zhao, and M. Yang. 2016. Node-grained incremental community detection for streaming networks. In *IEEE 28th International Conference on Tools with Artificial Intelligence (ICTAI)*. IEEE, 585–592.
- [71] Y. You, L. Ren, Z. Zhang, K. Zhang, and J. Huang. 2022. Research on improvement of Louvain community detection algorithm. In *2nd International Conference on Artificial Intelligence, Automation, and High-Performance Computing (AIAHPC)*, Vol. 12348. SPIE, Zhuhai, China, 527–531.
- [72] N. Zarayeneh and A. Kalyanaraman. 2021. Delta-Screening: A Fast and Efficient Technique to Update Communities in Dynamic Graphs. *IEEE transactions on network science and engineering* 8, 2 (Apr 2021), 1614–1629.
- [73] J. Zeng and H. Yu. 2015. Parallel Modularity-Based Community Detection on Large-Scale Graphs. In *IEEE International Conference on Cluster Computing*. IEEE, 1–10.
- [74] J. Zhang, J. Fei, X. Song, and J. Feng. 2021. An improved Louvain algorithm for community detection. *Mathematical Problems in Engineering* 2021 (2021), 1–14.
- [75] D. Zhuang, J. Chang, and M. Li. 2019. DynaMo: Dynamic community detection by incrementally maximizing modularity. *IEEE Transactions on Knowledge and Data Engineering* 33, 5 (2019), 1934–1945.

A APPENDIX

A.1 Our Parallel Naive-dynamic (ND) Louvain

Algorithm 2 presents our multicore implementation of Naive dynamic (ND) Louvain, where vertices are assigned to communities from the previous snapshot of the graph, and all vertices are processed irrespective of edge deletions and insertions in the batch update. Algorithm 2 requires several inputs, including the previous G^{t-1} and current graph snapshots G^t , edge deletions Δ^{t-} and insertions Δ^{t+} in the batch update, the previous community membership of each vertex C^{t-1} , weighted degree of each vertex K^{t-1} , and total edge weight of each community Σ^{t-1} . The output consists of the updated community memberships C^t , weighted-degrees K^t , and total edge weight of communities Σ^t .

In the algorithm, we start by defining two lambda functions for the Louvain algorithm, `isAffected()` (lines 3-4) and `inAffectedRange()` (lines 5-6), which indicate that all vertices in the graph G^t are to be marked as affected, and that all such vertices can be incrementally marked as affected, respectively. Unlike existing works, we then utilize K^{t-1} and Σ^{t-1} , along with the batch update Δ^{t-} and Δ^{t+} , to quickly obtain K^t and Σ^t which is needed in the local-moving phase of the Louvain algorithm (line 9). The lambda functions and the total vertex/edge weights are then used to run the Louvain algorithm, and obtain the updated community assignments C^t (line 11). Finally, C^t is returned, along with K^t and Σ^t as the updated auxiliary information (line 12).

A.2 Our Parallel Delta-screening (DS) Louvain

The pseudocode of our multicore implementation of Delta-screening (DS) Louvain is given in Algorithm 3. It uses modularity-based scoring to determine an approximate region of the graph in which vertices are likely to change their community membership [72]. The algorithm accepts as input the previous G^{t-1} and current snapshot of the graph G^t , edge deletions Δ^{t-} and insertions Δ^{t+} in the batch update, the previous community memberships of vertices C^{t-1} , weighted degrees of vertices K^{t-1} , and total edge weights of communities Σ^{t-1} . It outputs the updated community memberships C^t , weighted-degrees K^t , and total edge weights of communities Σ^t . The batch update, comprising edge deletions $(i, j, w) \in \Delta^{t-}$ and insertions $(i, j, w) \in \Delta^{t+}$, is sorted separately by their source vertex ID i beforehand, as a preprocessing step.

In the algorithm, we first initialize a hashtable H , mapping communities to their associated weights, and affected flags δV , δE , and δC , indicating if a vertex, its neighbors, or its community is affected by the batch update (lines 2). Then, we parallelly iterate over edge deletions Δ^{t-} and insertions Δ^{t+} . For each deletion $(i, j, w) \in \Delta^{t-}$ where i and j are in the same community, we mark the source vertex i , its neighbors, and its community as affected (lines 4-6). For each unique source vertex $i \mid (i, j, w) \in \Delta^{t+}$ in insertions belonging to different communities, we identify the community c^* with the highest delta-modularity if i moves to one of its neighboring communities and mark i , its neighbors, and the community c^* as affected (lines 7-13). Deletions between different communities and insertions within the same community are disregarded. Using affected neighbor δE and community flags δC , affected vertices in δV are marked (lines 14-19). Next, similar to ND Louvain, we use K^{t-1} and Σ^{t-1} , along with Δ^{t-} and Δ^{t+} , to quickly yield K^t

Algorithm 2 Our Parallel Naive-dynamic (ND) Louvain.

```

▷  $G^{t-1}, G^t$ : Previous, current input graph
▷  $\Delta^{t-}, \Delta^{t+}$ : Edge deletions and insertions (batch update)
▷  $C^{t-1}, C^t$ : Previous, current community of each vertex
▷  $K^{t-1}, K^t$ : Previous, current weighted-degree of vertices
▷  $\Sigma^{t-1}, \Sigma^t$ : Previous, current total edge weight of communities
□ isAffected(i): Is vertex  $i$  is marked as affected?
□ inAffectedRange(i): Can  $i$  be incrementally marked?
□  $F$ : Lambda functions passed to parallel Louvain (Alg. 4)

1: function NAIVEDYNAMIC( $G^{t-1}, G^t, \Delta^{t-}, \Delta^{t+}, C^{t-1}, K^{t-1}, \Sigma^{t-1}$ )
2:   ▷ Mark affected vertices
3:   function ISAFPECTED( $i$ )
4:     return 1
5:   function INAFPECTEDRANGE( $i$ )
6:     return 1
7:    $F \leftarrow \{\text{isAffected}, \text{inAffectedRange}\}$ 
8:   ▷ Use  $K^{t-1}, \Sigma^{t-1}$  as auxiliary information (Alg. 7)
9:    $\{K^t, \Sigma^t\} \leftarrow \text{updateWeights}(G^t, \Delta^{t-}, \Delta^{t+}, C^{t-1}, K^{t-1}, \Sigma^{t-1})$ 
10:  ▷ Obtain updated communities (Alg. 4)
11:   $C^t \leftarrow \text{louvain}(G^t, C^{t-1}, K^t, \Sigma^t, F)$ 
12:  return  $\{C^t, K^t, \Sigma^t\}$ 

```

and Σ^t (line 9), define the needed lambda functions `isAffected()` (lines 20-21) and `inAffectedRange()` (lines 22-23), and run the Louvain algorithm, yielding updated community assignments C^t (line 28). Finally, updated community memberships C^t are returned, alongside K^t and Σ^t as updated auxiliary information (line 29).

A.3 Our Dynamic-supporting Parallel Louvain

The main step of our Dynamic-supporting Parallel Louvain algorithm is given in Algorithm 4. Unlike our implementation of Static Louvain [56], in addition to the current graph snapshot G^t , it accepts as input the previous community membership of each vertex C^{t-1} , the updated weighted-degree of each vertex K^t , the updated total edge weight of each community Σ^t , and a set of lambda functions F which determine if a given vertex is affected, or if it can be incrementally marked as affected (it is in the affected range). It outputs the updated community memberships of vertices C^t .

In the algorithm, we commence by marking affected vertices as unprocessed (lines 3-4). Subsequently, the initialization phase follows, wherein we initialize the community membership of each vertex C in G^t . Additionally, we initialize the total edge weight of each vertex K^t , the total edge weight of each community Σ^t , and the community membership C' of each vertex in the current/super-vertex graph G' (lines 6-7). After initialization, we conduct a series of passes (lines 9-20) of the local-moving and aggregation phases (limited to `MAX_PASSES`). Within each pass, in line 10, we execute the local-moving phase of the Louvain algorithm (Algorithm 5), which optimizes community assignments. If the local-moving phase converges within a single iteration, it implies global convergence, prompting the termination of passes (line 11). Conversely, if the drop in community count $|\Gamma|$ is deemed insignificant, indicating diminishing returns, we halt at the current pass (line 13). Should the convergence conditions not be met, we progress to the aggregation

Algorithm 3 Our Parallel *Delta-screening* (DS) Louvain.

```

1:  $G^{t-1}, G^t$ : Previous, current input graph
2:  $\Delta^{t-}, \Delta^{t+}$ : Edge deletions and insertions (batch update)
3:  $C^{t-1}, C^t$ : Previous, current community of each vertex
4:  $K^{t-1}, K^t$ : Previous, current weighted-degree of vertices
5:  $\Sigma^{t-1}, \Sigma^t$ : Previous, current total edge weight of communities
6:  $\delta V, \delta E, \delta C$ : Is vertex, neighbors, or community affected?
7:  $H$ : Hashtable mapping a community to associated weight
8:  $isAffected(i)$ : Is vertex  $i$  is marked as affected?
9:  $inAffectedRange(i)$ : Can  $i$  be incrementally marked?
10:  $F$ : Lambda functions passed to parallel Louvain (Alg. 4)

1: function DELTASCREENING( $G^{t-1}, G^t, \Delta^{t-}, \Delta^{t+}, C^{t-1}, K^{t-1}, \Sigma^{t-1}$ )
2:    $H, \delta V, \delta E, \delta C \leftarrow \{\}$ 
3:    $\triangleright$  Mark affected vertices
4:   for all  $(i, j, w) \in \Delta^{t-}$  in parallel do
5:     if  $C^{t-1}[i] = C^{t-1}[j]$  then
6:        $\delta V[i], \delta E[i], \delta C[C^{t-1}[j]] \leftarrow 1$ 
7:   for all unique source vertex  $i \in \Delta^{t+}$  in parallel do
8:      $H \leftarrow \{\}$ 
9:     for all  $(i', j, w) \in \Delta^{t+} \mid i' = i$  do
10:      if  $C^{t-1}[i] \neq C^{t-1}[j]$  then
11:         $H[C^{t-1}[j]] \leftarrow H[C^{t-1}[j]] + w$ 
12:       $c^* \leftarrow$  Best community linked to  $i$  in  $H$ 
13:       $\delta V[i], \delta E[i], \delta C[c^*] \leftarrow 1$ 
14:     for all  $i \in V^t$  in parallel do
15:       if  $\delta E[i]$  then
16:         for all  $j \in G^t.neighbors(i)$  do
17:            $\delta V[j] \leftarrow 1$ 
18:         if  $\delta C[C^{t-1}[i]]$  then
19:            $\delta V[i] \leftarrow 1$ 
20:     function ISAFFFECTED( $i$ )
21:       return  $\delta V[i]$ 
22:     function INAFFFECTEDRANGE( $i$ )
23:       return  $\delta V[i]$ 
24:    $F \leftarrow \{isAffected, inAffectedRange\}$ 
25:    $\triangleright$  Use  $K^{t-1}, \Sigma^{t-1}$  as auxiliary information (Alg. 7)
26:    $\{K^t, \Sigma^t\} \leftarrow updateWeights(G^t, \Delta^{t-}, \Delta^{t+}, C^{t-1}, K^{t-1}, \Sigma^{t-1})$ 
27:    $\triangleright$  Obtain updated communities (Alg. 4)
28:    $C^t \leftarrow lowvain(G^t, C^{t-1}, K^t, \Sigma^t, F)$ 
29:   return  $\{C^t, K^t, \Sigma^t\}$ 

```

phase. Here, we renumber communities (line 14), update top-level community memberships C using dendrogram lookup (line 15), execute the aggregation phase (Algorithm 6), and adjust the convergence threshold for subsequent passes, i.e., perform threshold scaling (line 20). The subsequent pass commences in line 9. Following all passes, we do a final update of the top-level community membership C of each vertex in G^t via dendrogram lookup (line 21), before ultimately returning it (line 22).

A.3.1 Local-moving phase of our Parallel Louvain. The pseudocode detailing the local-moving phase of our Parallel Louvain algorithm is presented in Algorithm 5. This phase iteratively moves vertices among communities in order to maximize modularity. Here, the

Algorithm 4 Our Dynamic-supporting Parallel Louvain [56].

```

1:  $G^t$ : Current input graph
2:  $C^{t-1}$ : Previous community of each vertex
3:  $K^t$ : Current weighted-degree of each vertex
4:  $\Sigma^t$ : Current total edge weight of each community
5:  $F$ : Lambda functions passed to parallel Louvain
6:  $G'$ : Current/super-vertex graph.
7:  $C, C'$ : Current community of each vertex in  $G^t, G'$ 
8:  $K, K'$ : Current weighted-degree of each vertex in  $G^t, G'$ 
9:  $\Sigma, \Sigma'$ : Current total edge weight of each community in  $G^t, G'$ 
10:  $\tau, \tau_{agg}$ : Iteration, aggregation tolerance

1: function LOUVAIN( $G^t, C^{t-1}, K^t, \Sigma^t, F$ )
2:    $\triangleright$  Mark affected vertices as unprocessed
3:   for all  $i \in V^t$  do
4:     if  $F.isAffected(i)$  then Mark  $i$  as unprocessed
5:    $\triangleright$  Initialization phase
6:   Vertex membership:  $C \leftarrow [0..|V^t|)$ 
7:    $G' \leftarrow G^t; C' \leftarrow C^{t-1}; K' \leftarrow K^t; \Sigma' \leftarrow \Sigma^t$ 
8:    $\triangleright$  Local-moving and aggregation phases
9:   for all  $l_p \in [0..MAX_PASSES)$  do
10:     $l_i \leftarrow lowvainMove(G', C', K', \Sigma', F)$   $\triangleright$  Alg. 5
11:    if  $l_i \leq 1$  then break  $\triangleright$  Globally converged?
12:     $|\Gamma|, |\Gamma_{old}| \leftarrow$  Number of communities in  $C, C'$ 
13:    if  $|\Gamma|/|\Gamma_{old}| > \tau_{agg}$  then break  $\triangleright$  Low shrink?
14:     $C' \leftarrow$  Renumber communities in  $C'$ 
15:     $C \leftarrow$  Lookup dendrogram using  $C$  to  $C'$ 
16:     $G' \leftarrow$  Aggregate communities in  $G'$  using  $C'$   $\triangleright$  Alg. 6
17:     $\Sigma' \leftarrow K' \leftarrow$  Weight of each vertex in  $G'$ 
18:    Mark all vertices in  $G'$  as unprocessed
19:     $C' \leftarrow [0..|V'|)$ 
20:     $\tau \leftarrow \tau/TOLERANCE\_DROP$   $\triangleright$  Threshold scaling
21:     $C \leftarrow$  Lookup dendrogram using  $C$  to  $C'$ 
22:   return  $C$ 

```

$lowvainMove()$ function operates on the current graph G' , community membership C' , total edge weight of each vertex K' , total edge weight of each community Σ' , and a set of lambda functions as inputs, yielding the number of iterations performed l_i .

Lines 2-15 encapsulate the primary loop of the local-moving phase. In line 3, we initialize the total delta-modularity per iteration ΔQ . Subsequently, in lines 4-14, we concurrently iterate over unprocessed vertices. For each vertex i , we perform vertex pruning by marking i as processed (line 5). Next, we verify if i falls within the affected range (i.e., it is permitted to be incrementally marked as affected), and if not, we proceed to the next vertex (line 6). For each unskipped vertex i , we scan communities connected to i (line 7), excluding itself, ascertain the optimal community c^* to move i to (line 9), compute the delta-modularity of moving i to c^* (line 10), update the community membership of i (lines 12-13), and mark its neighbors as unprocessed (line 14) if a superior community is identified. It's worth noting that this practice of marking neighbors of i as unprocessed, which is part of the vertex pruning optimization, also aligns with algorithm of DF Louvain — which marks its neighbors as affected, when a vertex changes its community.

Algorithm 5 Local-moving phase of our Parallel Louvain [56].

```

▷  $G'$ : Input/super-vertex graph
▷  $C'$ : Community membership of each vertex
▷  $K'$ : Total edge weight of each vertex
▷  $\Sigma'$ : Total edge weight of each community
▷  $F$ : Lambda functions passed to parallel Louvain
□  $H_t$ : Collision-free per-thread hashtable
□  $l_i$ : Number of iterations performed
□  $\tau$ : Per iteration tolerance

1: function LOUVAINMOVE( $G', C', K', \Sigma', F$ )
2:   for all  $l_i \in [0..MAX\_ITERATIONS]$  do
3:     Total delta-modularity per iteration:  $\Delta Q \leftarrow 0$ 
4:     for all unprocessed  $i \in V'$  in parallel do
5:       Mark  $i$  as processed (prune)
6:       if not  $F.inAffectedRange(i)$  then continue
7:        $H_t \leftarrow scanCommunities(\{i\}, G', C', i, false)$ 
8:       ▷ Use  $H_t, K', \Sigma'$  to choose best community
9:        $c^* \leftarrow$  Best community linked to  $i$  in  $G'$ 
10:       $\delta Q^* \leftarrow$  Delta-modularity of moving  $i$  to  $c^*$ 
11:      if  $c^* = C'[i]$  then continue
12:       $\Sigma'[C'[i]] - = K'[i]; \Sigma'[c^*] + = K'[i]$  atomic
13:       $C'[i] \leftarrow c^*; \Delta Q \leftarrow \Delta Q + \delta Q^*$ 
14:      Mark neighbors of  $i$  as unprocessed
15:      if  $\Delta Q \leq \tau$  then break           ▷ Locally converged?
16:   return  $l_i$ 

17: function SCANCOMMUNITIES( $H_t, G', C', i, self$ )
18:   for all  $(j, w) \in G'.edges(i)$  do
19:     if  $self$  or  $i \neq j$  then  $H_t \leftarrow H_t[C'[j]] + w$ 
20:   return  $H_t$ 

```

Thus, vertex pruning facilitates incremental expansion of the set of affected vertices without requiring any extra code. In line 15, we examine whether the local-moving phase has achieved convergence (locally); if so, the loop is terminated (or if `MAX_ITERATIONS` is reached). Finally, in line 16, we return the number of iterations performed by the local-moving phase l_i .

A.3.2 Aggregation phase of our Parallel Louvain. Finally, the pseudocode for the aggregation phase is depicted in Algorithm 6, where communities are amalgamated into super-vertices. Here, the `LouvainAggregate()` function receives the current graph G' and the community membership C' , and yields the super-vertex graph G'' .

In the algorithm, we begin by obtaining the offsets array for the community vertices CSR $G'_{C'}.offsets$ in lines 3-4. This involves first counting the number of vertices belonging to each community using `countCommunityVertices()`, followed by performing an exclusive scan operation on the array. Subsequently, in lines 5-6, we concurrently iterate over all vertices, atomically populating vertices associated with each community into the community graph CSR $G'_{C'}$. Next, we derive the offsets array for the super-vertex graph CSR by overestimating the degree of each super-vertex in lines 8-9, by computing the total degree of each community using `communityTotalDegree()` and then performing an exclusive

Algorithm 6 Aggregation phase of our Parallel Louvain [56].

```

▷  $G'$ : Input/super-vertex graph
▷  $C'$ : Community membership of each vertex
□  $G'_{C'}$ : Community vertices (CSR)
□  $G''$ : Super-vertex graph (weighted CSR)
□  $*.offsets$ : Offsets array of a CSR graph
□  $H_t$ : Collision-free per-thread hashtable

1: function LOUVAINAGGREGATE( $G', C'$ )
2:   ▷ Obtain vertices belonging to each community
3:    $G'_{C'}.offsets \leftarrow countCommunityVertices(G', C')$ 
4:    $G'_{C'}.offsets \leftarrow exclusiveScan(G'_{C'}.offsets)$ 
5:   for all  $i \in V'$  in parallel do
6:     Add edge  $(C'[i], i)$  to CSR  $G'_{C'}$  atomically
7:   ▷ Obtain super-vertex graph
8:    $G''.offsets \leftarrow communityTotalDegree(G', C')$ 
9:    $G''.offsets \leftarrow exclusiveScan(G''.offsets)$ 
10:   $|\Gamma| \leftarrow$  Number of communities in  $C'$ 
11:  for all  $c \in [0, |\Gamma|)$  in parallel do
12:    if degree of  $c$  in  $G'_{C'} = 0$  then continue
13:     $H_t \leftarrow \{i\}$ 
14:    for all  $i \in G'_{C'}.edges(c)$  do
15:       $H_t \leftarrow scanCommunities(H, G', C', i, true)$ 
16:    for all  $(d, w) \in H_t$  do
17:      Add edge  $(c, d, w)$  to CSR  $G''$  atomically
18:  return  $G''$ 

```

scan on the array. As a result, the super-vertex graph CSR exhibits holes/intervals between the edges and weights array of each super-vertex. Following this, in lines 11-17, we iterate over all communities $c \in [0, |\Gamma|)$. Here, we add all communities d (along with their associated edge weight w) linked to each vertex i belonging to community c (via `scanCommunities()` defined in Algorithm 5) to the per-thread hashtable H_t . Once H_t encompasses all communities (alongside their weights) linked to community c , we atomically append them as edges to super-vertex c within the super-vertex graph G'' . Finally, in line 18, we return the super-vertex graph G'' .

A.4 Updating vertex/community weights

We now discuss the parallel algorithm for obtaining the updated weighted degree of each vertex K^t and total edge weight of each community Σ^t , given the previous community memberships of vertices C^{t-1} , weighted-degrees of vertices K^{t-1} , total edge weights of communities, and the batch update (consisting of edge deletions Δ^{t-} and insertions Δ^{t+}). Its pseudocode is in Algorithm 7.

In the algorithm, we begin by initializing K and Σ , the weighted-degree of each vertex, and the total edge weight of each community (line 2). Then, across multiple threads, we iterate over both the sets of edge deletions Δ^{t-} (lines 3-7) and edge insertions Δ^{t+} (lines 8-11). For each edge deletion (i, j, w) in Δ^{t-} , we determine the community c of vertex i based on the previous community assignment C^{t-1} (line 5). If i belongs to the current thread's work-list, we decrement its weighted-degree by w (line 6), and if community c belongs to the work-list, we decrement its total edge weight by w (line 7).

Algorithm 7 Updating vertex/community weights in parallel.

$\triangleright G^t$: Current input graph
 $\triangleright \Delta^{t-}, \Delta^{t+}$: Edge deletions and insertions (batch update)
 $\triangleright C^{t-1}$: Previous community of each vertex
 $\triangleright K^{t-1}$: Previous weighted-degree of each vertex
 $\triangleright \Sigma^{t-1}$: Previous total edge weight of each community
 $\square K$: Updated weighted-degree of each vertex
 $\square \Sigma$: Updated total edge weight of each community
 $\square work_{th}$: Work-list of current thread

```

1: function UPDATEWEIGHTS( $G^t, \Delta^{t-}, \Delta^{t+}, C^{t-1}, K^{t-1}, \Sigma^{t-1}$ )
2:    $K \leftarrow K^{t-1}; \Sigma \leftarrow \Sigma^{t-1}$ 
3:   for all threads in parallel do
4:     for all  $(i, j, w) \in \Delta^{t-}$  do
5:        $c \leftarrow C^{t-1}[i]$ 
6:       if  $i \in work_{th}$  then  $K[i] \leftarrow K[i] - w$ 
7:       if  $c \in work_{th}$  then  $\Sigma[c] \leftarrow \Sigma[c] - w$ 
8:     for all  $(i, j, w) \in \Delta^{t+}$  do
9:        $c \leftarrow C^{t-1}[i]$ 
10:      if  $i \in work_{th}$  then  $K[i] \leftarrow K[i] + w$ 
11:      if  $c \in work_{th}$  then  $\Sigma[c] \leftarrow \Sigma[c] + w$ 
12:   return  $\{K, \Sigma\}$ 
  
```

Similarly, for each edge insertion (i, j, w) in Δ^{t+} , we adjust the vertex i 's weighted-degree and its community's total edge weight accordingly. Finally, we return the updated values of K and Σ for each vertex and community for further processing (line 12).

A.5 Correctness of DF Louvain

We now provide arguments for the correctness of Dynamic Frontier (DF) Louvain. To help with this, we refer the reader to Figure 10. Here, pre-existing edges are represented by solid lines, and i represents a source vertex of edge deletions/insertions in the batch update. Edge deletions in the batch update with i as the source vertex are shown in the top row (denoted by dashed lines), edge insertions are shown in the middle row (also denoted by dashed lines), and community migration of vertex i is shown in the bottom row. Vertices i_n and j_n represent the destination vertices (of edge deletions or insertions). Vertices i', j' , and k' signify neighboring vertices of vertex i . Finally, vertices i'', j'' , and k'' represent non-neighbor vertices (to vertex i). Yellow highlighting is used to indicate vertices marked as affected, initially or in the current iteration of the Louvain algorithm.

Given a batch update consisting of edge deletions Δ^{t-} and insertions Δ^{t+} , we now show that DF Louvain marks the essential vertices, which have an incentive to change their community membership, as affected. For any given vertex i in the original graph (before the batch update), the delta-modularity of moving it from its current community d to a new community c is given by Equation 3. We now consider the direct effect of each individual edge deletion (i, j) or insertion (i, j, w) in the batch update, on the delta-modularity of the a vertex, as well as the indirect cascading effect of migration of a vertex (to another community) on other vertices.

$$\Delta Q_{i:d \rightarrow c} = \frac{1}{m} (K_{i \rightarrow c} - K_{i \rightarrow d}) - \frac{K_i}{2m^2} (K_i + \Sigma_c - \Sigma_d) \quad (3)$$

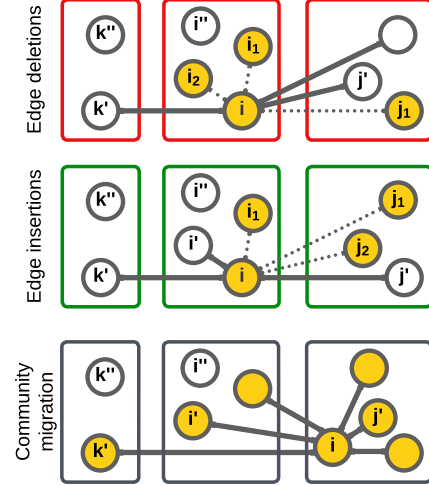


Figure 10: A detailed illustration for presenting arguments on the correctness of Dynamic Frontier (DF) Louvain.

A.5.1 On edge deletion.

LEMMA A.1. *Given an edge deletion (i, j) between vertices i and j belonging to the same community d , vertex i (and j) should be marked as affected.*

Consider the case of edge deletion (i, j) of weight w between vertices i and j belonging to the same community $C_i = C_j = d$ (see Figure 10, where $j = i_1$). Let i'' be a vertex belonging to i 's community $C_{i''} = d$, and let k'' be a vertex belonging to another community $C_{k''} = b$. As shown below in Case (1), the delta-modularity of vertex i moving from its original community d to another community b has a significant positive factor w/m . There is thus a chance that vertex i would change its community membership, and we should mark it as affected. The same argument applies for vertex j , as the edge is undirected. On the other hand, for the Cases (2)-(3), there is only a small positive change in delta-modularity for vertex k'' . Thus, there is little incentive for vertex k'' to change its community membership, and no incentive for a change in community membership of vertex i'' .

Note that it is possible that the community d would split due to the edge deletion. However, this is unlikely, given that one would need a large number of edge deletions between vertices belonging to the same community for the community to split. One can take care of such rare events by running Static Louvain, say every 1000 batch updates, which also helps us ensure high-quality communities. The same applies to Delta-screening (DS) Louvain.

- (1) $\Delta Q_{i:d \rightarrow b}^{new} = \Delta Q_{i:d \rightarrow b} + \left\lceil \frac{w}{m} \right\rceil + \frac{w}{2m^2} (\Sigma_c - \Sigma_d + w)$
- (2) $\Delta Q_{i'':d \rightarrow b}^{new} = \Delta Q_{i'':d \rightarrow b} - \frac{wK_{i''}}{m^2}$
- (3) $\Delta Q_{k'':b \rightarrow d}^{new} = \Delta Q_{k'':b \rightarrow d} + \frac{wK_{k''}}{m^2}$

Now, consider the case of edge deletion (i, j) between vertices i and j belonging to different communities, i.e., $C_i = d$, $C_j = c$ (see Figure 10, where $j = j_2$ or j_3). Let i'' be a vertex belonging to i 's community $C_{i''} = d$, j'' be a vertex belonging to j 's community $C_{j''} = c$, and k'' be a vertex belonging another community $C_{k''} = b$. As shown in Cases (4)-(8), due to the absence of any significant positive change in delta-modularity, there is little to no incentive for vertices i , j , k'' , i'' , and j'' to change their community membership.

$$\begin{aligned} (4) \quad \Delta Q_{i:d \rightarrow c}^{new} &= \Delta Q_{i:d \rightarrow c} - \frac{w}{m} + \frac{w}{2m^2} (2K_i + \Sigma_c - \Sigma_d - w) \\ (5) \quad \Delta Q_{i:d \rightarrow b}^{new} &= \Delta Q_{i:d \rightarrow b} + \frac{w}{2m^2} (K_i + \Sigma_b - \Sigma_d) \\ (6) \quad \Delta Q_{i'':d \rightarrow c}^{new} &= \Delta Q_{i'':d \rightarrow c} \\ (7) \quad \Delta Q_{i'':d \rightarrow b}^{new} &= \Delta Q_{i'':d \rightarrow b} - \frac{wK_{i''}}{2m^2} \\ (8) \quad \Delta Q_{k'':b \rightarrow d/c}^{new} &= \Delta Q_{k'':b \rightarrow d/c} + \frac{wK_{k''}}{m^2} \quad \diamond \end{aligned}$$

A.5.2 On edge insertion.

LEMMA A.2. *Given an edge insertion (i, j, w) between vertices i and j belonging to different communities d and c , vertex i (and j) should be marked as affected.*

Let us consider the case of edge insertion (i, j, w) between vertices i and j belonging to different communities $C_i = d$ and $C_j = c$ respectively (see Figure 10, where $j = j_3$). Let i'' be a vertex belonging to i 's community $C_{i''} = d$, j'' be a vertex belonging to j 's community $C_{j''} = c$, and k'' be a vertex belonging to another community $C_{k''} = b$. As shown below in Case (9), we have a significant positive factor w/m (and a small negative factor) which increases the delta-modularity of vertex i moving to j 's community after the insertion of the edge (i, j) . There is, therefore, incentive for vertex i to change its community membership. Accordingly, we mark i as affected. Again, the same argument applies for vertex j , as the edge is undirected. Further, we observe from other Cases (10)-(13) there is only a small change in delta-modularity. Thus, there is hardly any to no incentive for a change in community membership of vertices i'' , j'' , and k'' .

$$\begin{aligned} (9) \quad \Delta Q_{i:d \rightarrow c}^{new} &= \Delta Q_{i:d \rightarrow c} + \left[\frac{w}{m} \right] - \frac{w}{2m^2} (2K_i + \Sigma_c - \Sigma_d + w) \\ (10) \quad \Delta Q_{i:d \rightarrow b}^{new} &= \Delta Q_{i:d \rightarrow b} - \frac{w}{2m^2} (K_i + \Sigma_b - \Sigma_d) \\ (11) \quad \Delta Q_{i'':d \rightarrow c}^{new} &= \Delta Q_{i'':d \rightarrow c} \\ (12) \quad \Delta Q_{i'':d \rightarrow b}^{new} &= \Delta Q_{i'':d \rightarrow b} + \frac{wK_{i''}}{2m^2} \\ (13) \quad \Delta Q_{k'':b \rightarrow d/c}^{new} &= \Delta Q_{k'':b \rightarrow d/c} - \frac{wK_{k''}}{2m^2} \end{aligned}$$

Now, consider the case of edge insertion (i, j, w) between vertices i and j belonging to the same community $C_i = C_j = d$ (see Figure 10, where $j = i_1$ or i_2). From Cases (14)-(16), we note that it is little to no incentive for vertices i'' , k'' , i , and j to change their community membership. Note that it is possible for the insertion of edges within the same community to cause it to split into two more strongly connected communities, but it is very unlikely.

$$\begin{aligned} (14) \quad \Delta Q_{i:d \rightarrow b}^{new} &= \Delta Q_{i:d \rightarrow b} - \frac{w}{m} - \frac{w}{2m^2} (\Sigma_c - \Sigma_d - w) \\ (15) \quad \Delta Q_{i'':d \rightarrow b}^{new} &= \Delta Q_{i'':d \rightarrow b} + \frac{wK_{i''}}{m^2} \\ (16) \quad \Delta Q_{k'':b \rightarrow d}^{new} &= \Delta Q_{k'':b \rightarrow d} - \frac{wK_{k''}}{m^2} \quad \diamond \end{aligned}$$

A.5.3 On vertex migration to another community.

LEMMA A.3. *When a vertex i changes its community membership, and vertex j is its neighbor, j should be marked as affected.*

We considered the direct effects of deletion and insertion of edges above. Now we consider its indirect effects by studying the impact of change in community membership of one vertex on the other vertices. Consider the case where a vertex i changes its community membership from its previous community d to a new community c (see Figure 10). Let i' be a neighbor of i and i'' be a non-neighbor of i belonging to i 's previous community $C_{i'} = C_{i''} = d$, j' be a neighbor of i and j'' be a non-neighbor of i belonging to i 's new community $C_{j'} = C_{j''} = c$, k' be a neighbor of i and k'' be a non-neighbor of i belonging to another community $C_{k'} = C_{k''} = b$. From Cases (17)-(22), we note that neighbors i' and k' have an incentive to change their community membership (as thus necessitate marking), but not j' . However, to keep the algorithm simple, we simply mark all the neighbors of vertex i as affected.

$$\begin{aligned} (17) \quad \Delta Q_{i':d \rightarrow c}^{new} &= \Delta Q_{i':d \rightarrow c} + \left[\frac{2w_{ij'}}{m} \right] - \frac{K_i K_{j'}}{m^2} \\ (18) \quad \Delta Q_{i':d \rightarrow b}^{new} &= \Delta Q_{i':d \rightarrow b} + \left[\frac{w_{ij'}}{m} \right] - \frac{K_i K_{j'}}{2m^2} \\ (19) \quad \Delta Q_{j':c \rightarrow d}^{new} &= \Delta Q_{j':c \rightarrow d} - \frac{2w_{ij'}}{m} + \frac{K_i K_{j'}}{m^2} \\ (20) \quad \Delta Q_{j':c \rightarrow b}^{new} &= \Delta Q_{j':c \rightarrow b} - \frac{w_{ij'}}{m} + \frac{K_i K_{j'}}{2m^2} \\ (21) \quad \Delta Q_{k':b \rightarrow d}^{new} &= \Delta Q_{k':b \rightarrow d} - \frac{w_{ik'}}{m} + \frac{K_i K_{k'}}{2m^2} \\ (22) \quad \Delta Q_{k':b \rightarrow c}^{new} &= \Delta Q_{k':b \rightarrow c} + \left[\frac{w_{ik'}}{m} \right] - \frac{K_i K_{k'}}{2m^2} \end{aligned}$$

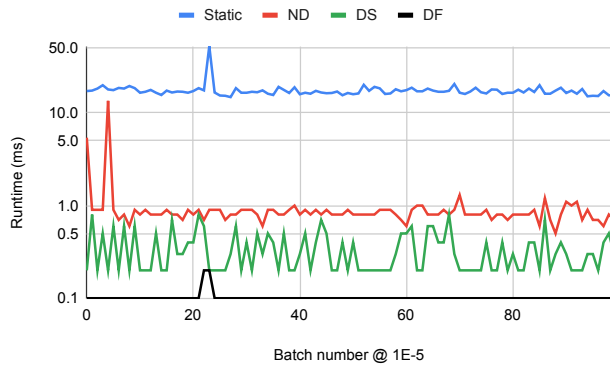
Further, from Cases (23)-(28), we note that there is hardly any incentive for a change in community membership of vertices i'' , j'' , and k'' . This is due to the change in delta-modularity being insignificant. There could still be an indirect cascading impact, where a common neighbor between vertices i and j would change its community, which could eventually cause vertex j to change its community as well [72]. However, this case is automatically taken care of as we perform marking of affected vertices during the community detection process.

$$\begin{aligned} (23) \quad \Delta Q_{i'':d \rightarrow c}^{new} &= \Delta Q_{i'':d \rightarrow c} + \frac{K_i K_{j''}}{m^2} \\ (24) \quad \Delta Q_{i'':d \rightarrow b}^{new} &= \Delta Q_{i'':d \rightarrow b} - \frac{K_i K_{j''}}{2m^2} \\ (25) \quad \Delta Q_{j'':c \rightarrow d}^{new} &= \Delta Q_{j'':c \rightarrow d} + \frac{K_i K_{j''}}{m^2} \\ (26) \quad \Delta Q_{j'':c \rightarrow b}^{new} &= \Delta Q_{j'':c \rightarrow b} + \frac{K_i K_{j''}}{2m^2} \\ (27) \quad \Delta Q_{k'':b \rightarrow d}^{new} &= \Delta Q_{k'':b \rightarrow d} + \frac{K_i K_{k''}}{2m^2} \\ (28) \quad \Delta Q_{k'':b \rightarrow c}^{new} &= \Delta Q_{k'':b \rightarrow c} - \frac{K_i K_{k''}}{2m^2} \quad \diamond \end{aligned}$$

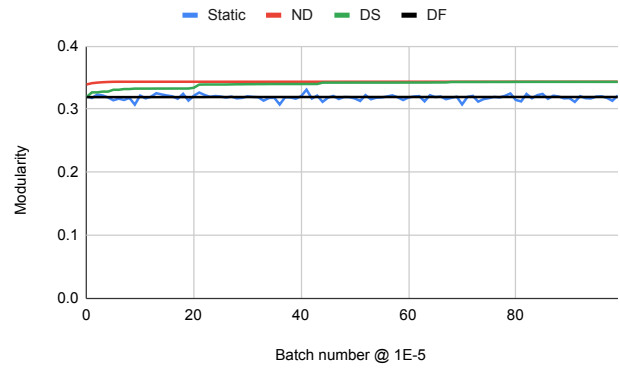
A.5.4 Overall. Finally, based on Lemmas A.1, A.2, and A.3, we can state the following for DF Louvain.

THEOREM A.4. *Given a batch update, DF Louvain marks vertices having an incentive to change their community as affected.* \square

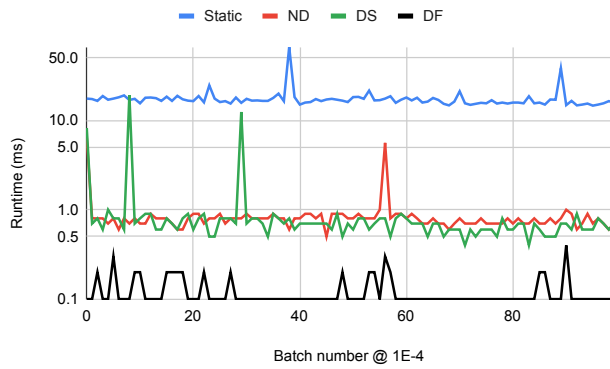
We note that with DF Louvain, without any direct link to vertices in the frontier, outlier vertices may not be marked as affected – even if they have the potential to change community. Such outliers may be weakly connected to multiple communities, and if the current community becomes weakly (or less strongly) connected, they may leave and join some other community. It may also be noted that DS Louvain is also an approximate method and can miss certain outliers. In practice, however, we see little to no impact of this approximation of the affected subset of the graph on the final quality (modularity) of the communities obtained, as shown in Section 5.



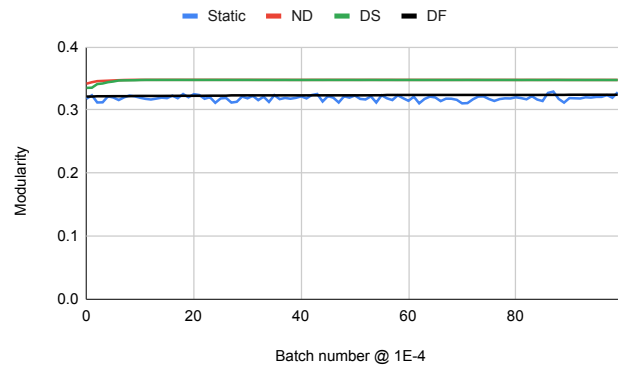
(a) Runtime on consecutive batch updates of size $10^{-5}|E_T|$



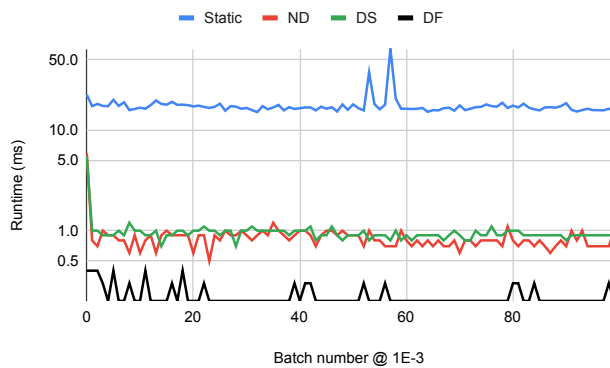
(b) Modularity of communities obtained on consecutive batch updates of size $10^{-5}|E_T|$



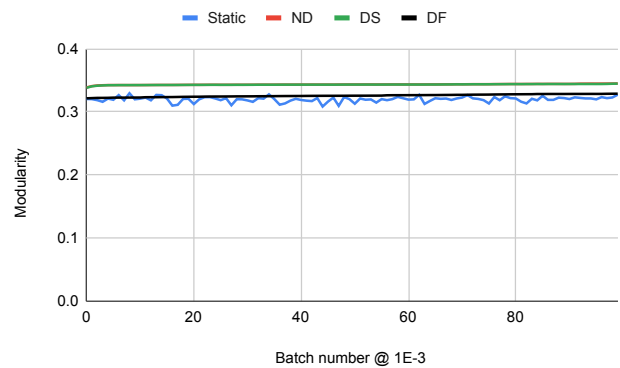
(c) Runtime on consecutive batch updates of size $10^{-4}|E_T|$



(d) Modularity of communities obtained on consecutive batch updates of size $10^{-4}|E_T|$

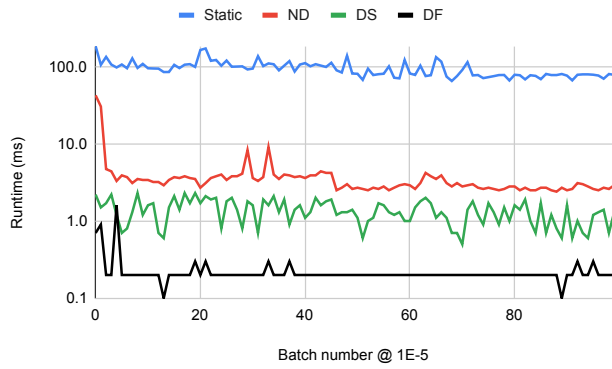


(e) Runtime on consecutive batch updates of size $10^{-3}|E_T|$

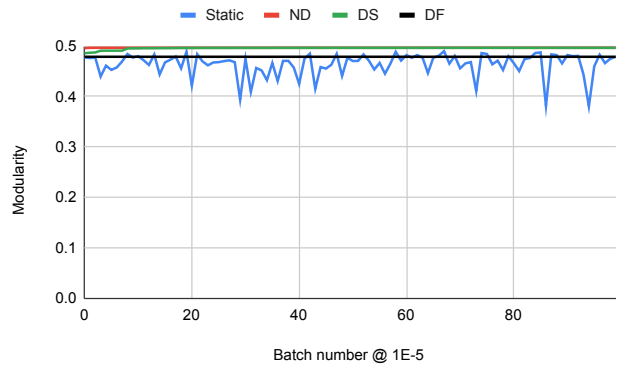


(f) Modularity of communities obtained on consecutive batch updates of size $10^{-3}|E_T|$

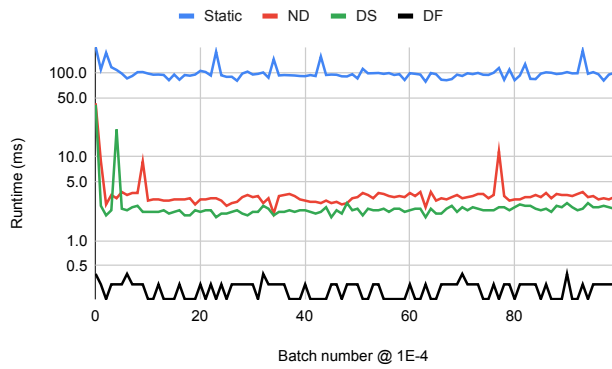
Figure 11: Runtime and Modularity of communities obtained with *Static*, *Naive-dynamic (ND)*, *Delta-screening (DS)*, and *Dynamic Frontier (DF)* Louvain on the *sx-mathoverflow* dynamic graph. The size of batch updates range from $10^{-5}|E_T|$ to $10^{-3}|E_T|$.



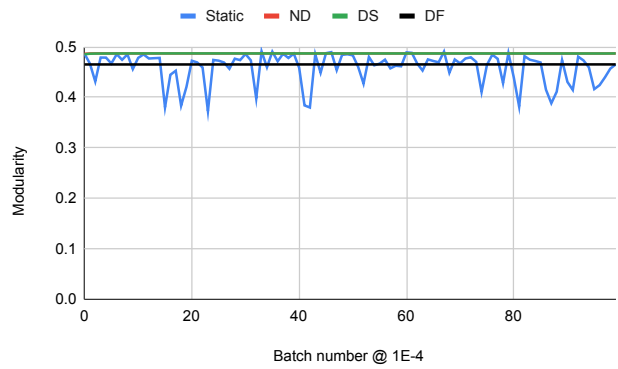
(a) Runtime on consecutive batch updates of size $10^{-5}|E_T|$



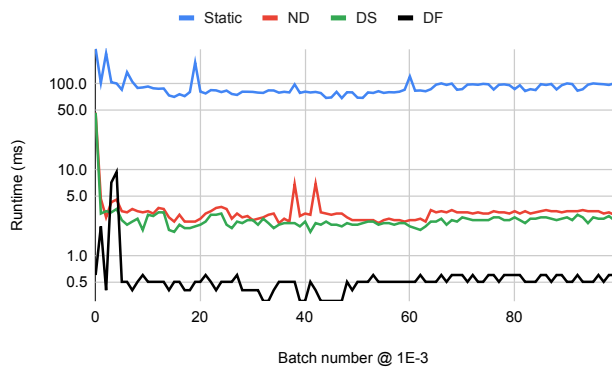
(b) Modularity of communities obtained on consecutive batch updates of size $10^{-5}|E_T|$



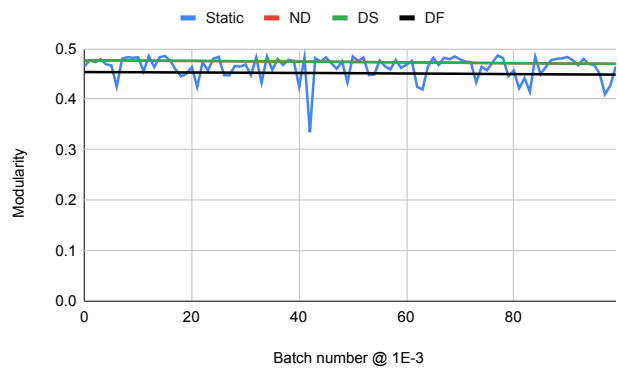
(c) Runtime on consecutive batch updates of size $10^{-4}|E_T|$



(d) Modularity of communities obtained on consecutive batch updates of size $10^{-4}|E_T|$

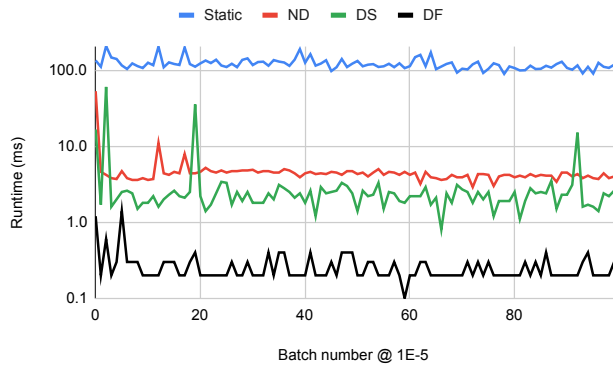


(e) Runtime on consecutive batch updates of size $10^{-3}|E_T|$

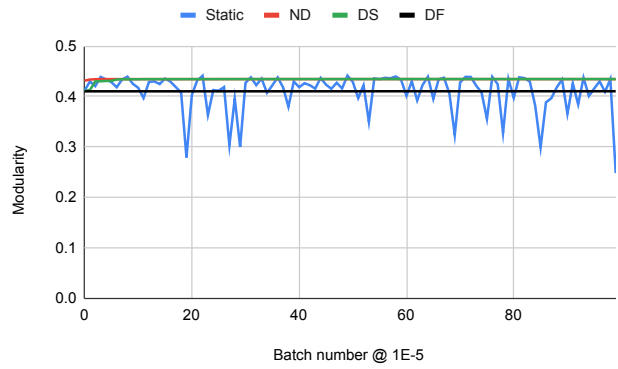


(f) Modularity of communities obtained on consecutive batch updates of size $10^{-3}|E_T|$

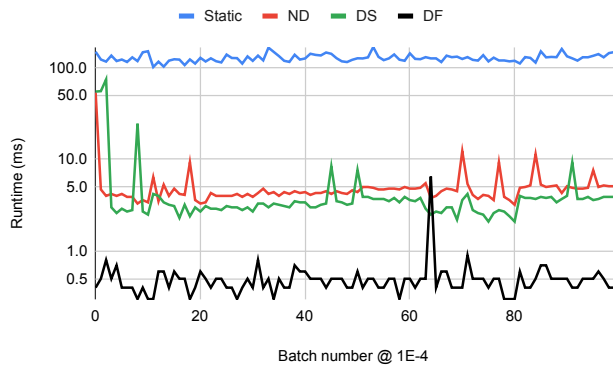
Figure 12: Runtime and Modularity of communities obtained with *Static*, *Naive-dynamic (ND)*, *Delta-screening (DS)*, and *Dynamic Frontier (DF)* Louvain on the *sx-askubuntu* dynamic graph. The size of batch updates range from $10^{-5}|E_T|$ to $10^{-3}|E_T|$.



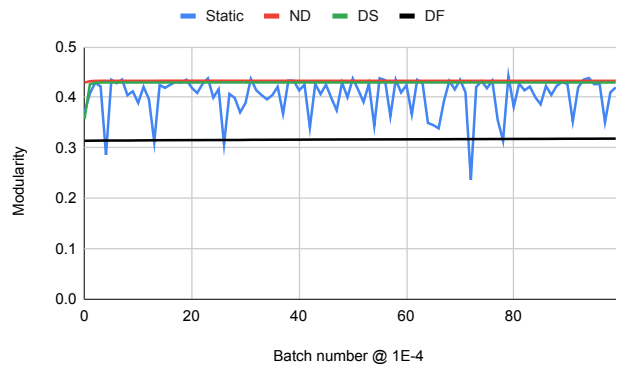
(a) Runtime on consecutive batch updates of size $10^{-5}|E_T|$



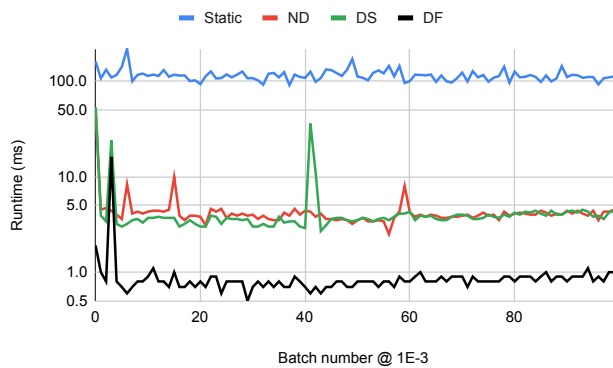
(b) Modularity of communities obtained on consecutive batch updates of size $10^{-5}|E_T|$



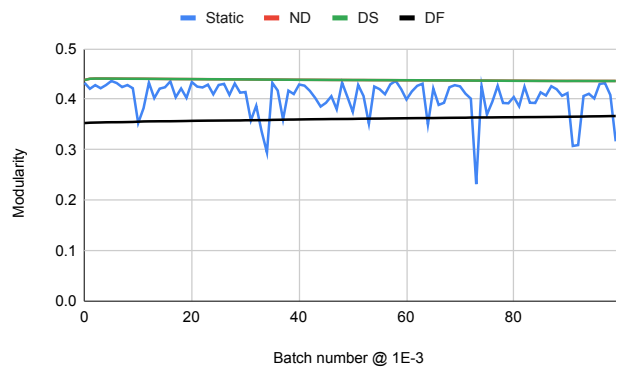
(c) Runtime on consecutive batch updates of size $10^{-4}|E_T|$



(d) Modularity of communities obtained on consecutive batch updates of size $10^{-4}|E_T|$

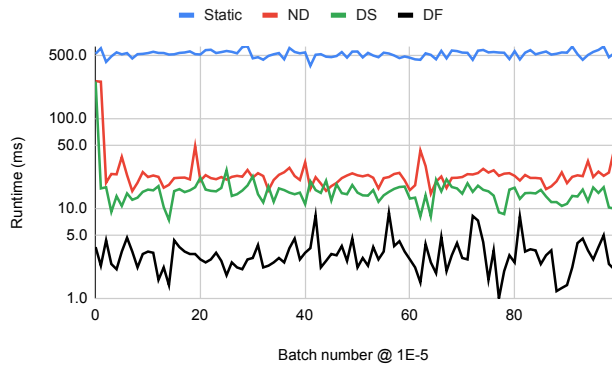


(e) Runtime on consecutive batch updates of size $10^{-3}|E_T|$

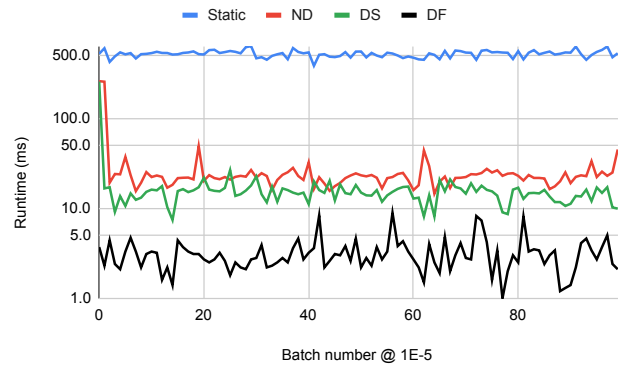


(f) Modularity of communities obtained on consecutive batch updates of size $10^{-3}|E_T|$

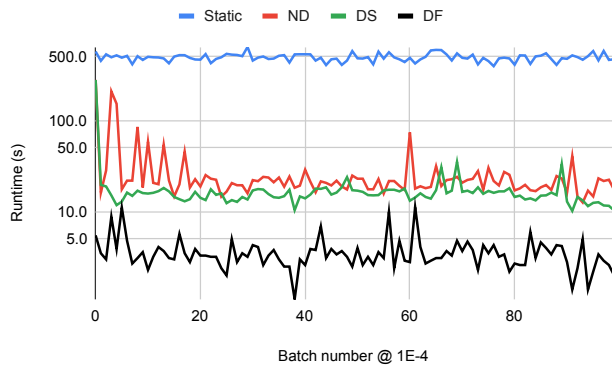
Figure 13: Runtime and Modularity of communities obtained with *Static*, *Naive-dynamic (ND)*, *Delta-screening (DS)*, and *Dynamic Frontier (DF)* Louvain on the *sx-superuser* dynamic graph. The size of batch updates range from $10^{-5}|E_T|$ to $10^{-3}|E_T|$.



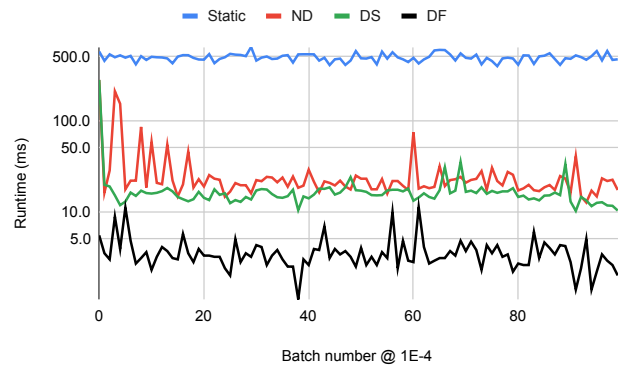
(a) Runtime on consecutive batch updates of size $10^{-5}|E_T|$



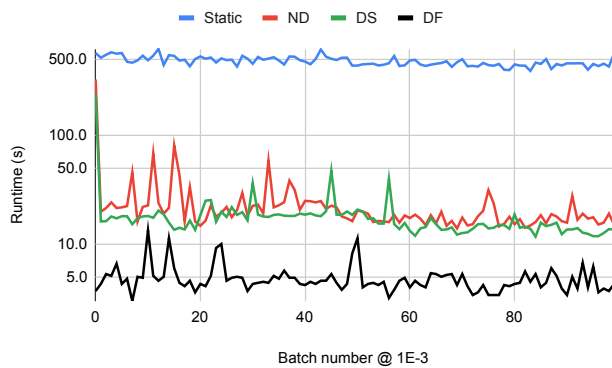
(b) Modularity of communities obtained on consecutive batch updates of size $10^{-5}|E_T|$



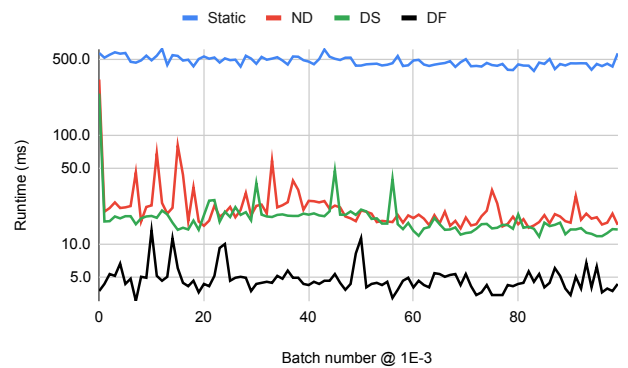
(c) Runtime on consecutive batch updates of size $10^{-4}|E_T|$



(d) Modularity of communities obtained on consecutive batch updates of size $10^{-4}|E_T|$

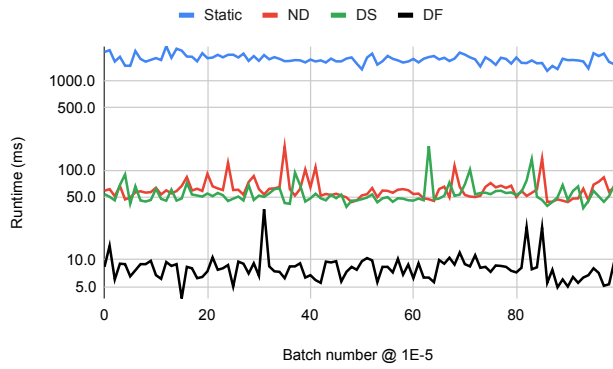


(e) Runtime on consecutive batch updates of size $10^{-3}|E_T|$

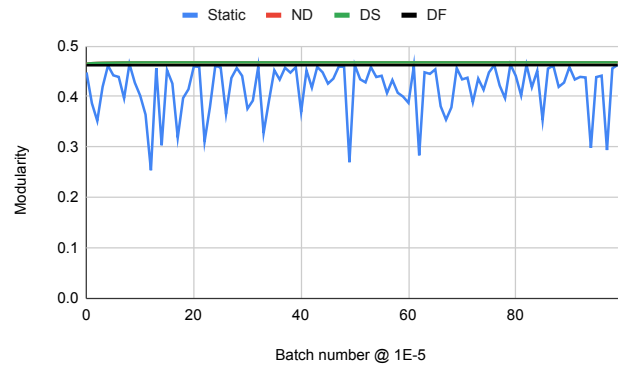


(f) Modularity of communities obtained on consecutive batch updates of size $10^{-3}|E_T|$

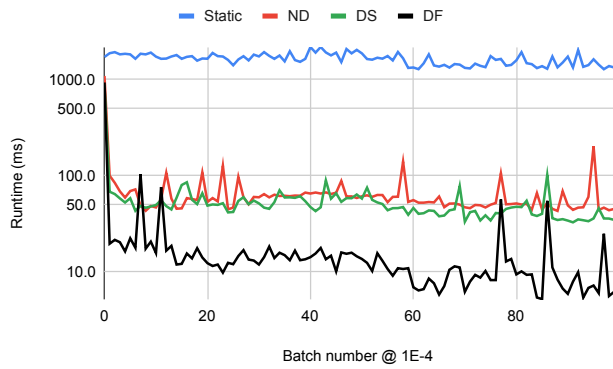
Figure 14: Runtime and Modularity of communities obtained with *Static*, *Naive-dynamic (ND)*, *Delta-screening (DS)*, and *Dynamic Frontier (DF)* Louvain on the *wiki-talk-temporal* dynamic graph. The size of batch updates range from $10^{-5}|E_T|$ to $10^{-3}|E_T|$.



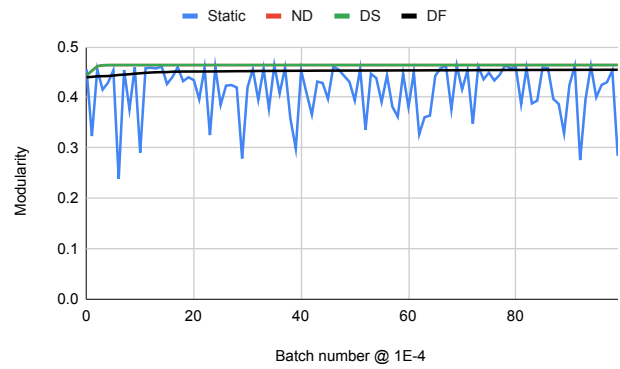
(a) Runtime on consecutive batch updates of size $10^{-5}|E_T|$



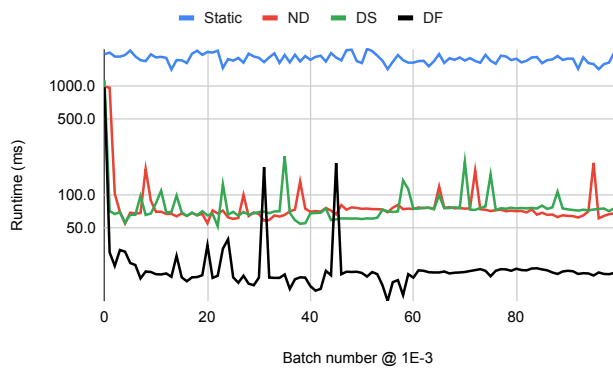
(b) Modularity of communities obtained on consecutive batch updates of size $10^{-5}|E_T|$



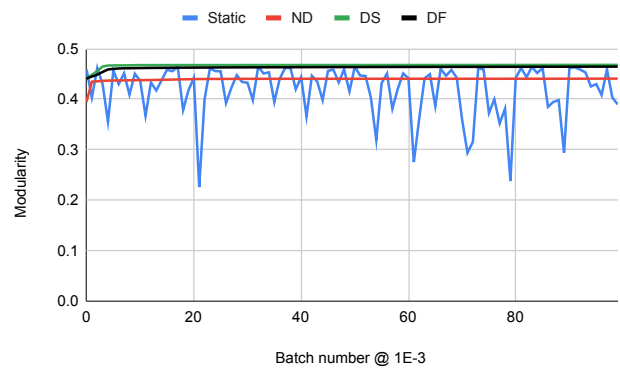
(c) Runtime on consecutive batch updates of size $10^{-4}|E_T|$



(d) Modularity of communities obtained on consecutive batch updates of size $10^{-4}|E_T|$



(e) Runtime on consecutive batch updates of size $10^{-3}|E_T|$



(f) Modularity of communities obtained on consecutive batch updates of size $10^{-3}|E_T|$

Figure 15: Runtime and Modularity of communities obtained with *Static*, *Naive-dynamic (ND)*, *Delta-screening (DS)*, and *Dynamic Frontier (DF)* Louvain on the *sx-stackoverflow* dynamic graph. The size of batch updates range from $10^{-5}|E_T|$ to $10^{-3}|E_T|$.